

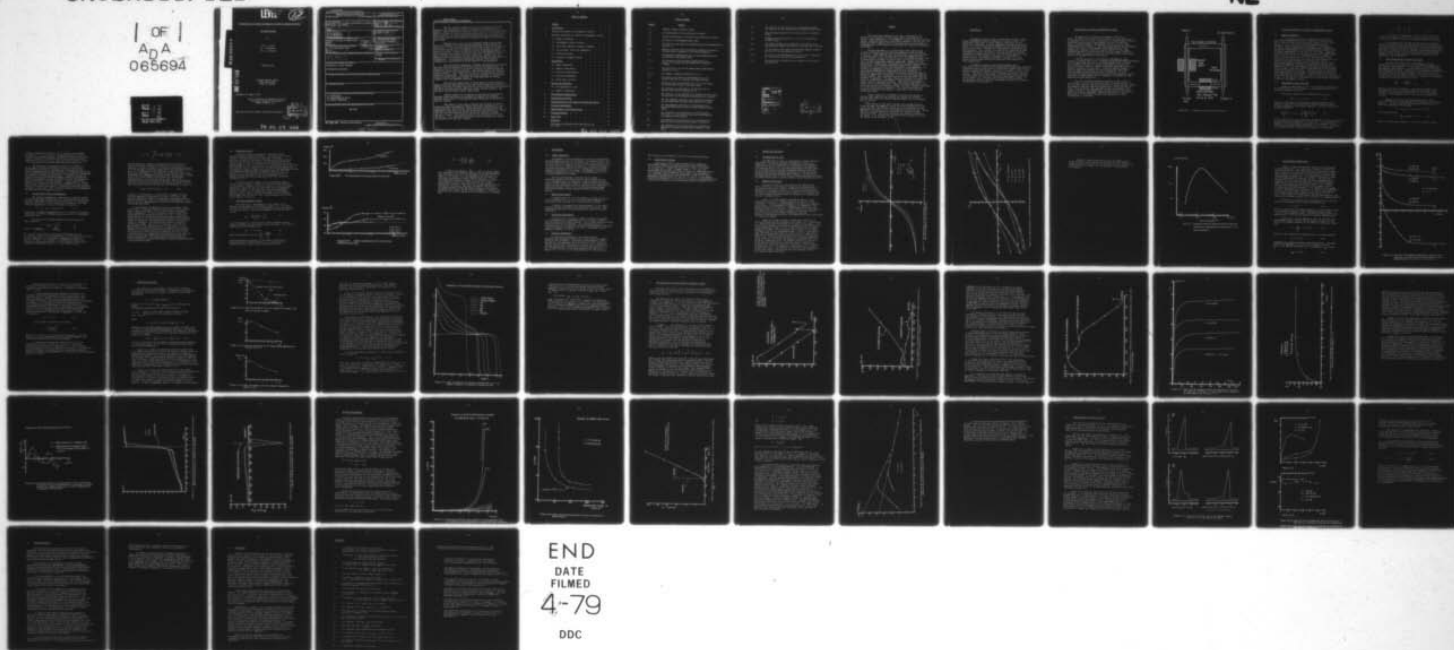
AD-A065 694

UNIVERSITY COLL OF NORTH WALES BANGOR SCHOOL OF PHYS--ETC F/6 20/3
THE PRODUCTION OF STABLE FERROMAGNETIC LIQUIDS FOR ENERGY CONVE--ETC(U)
NOV 78 S R HOON, J POPPLEWELL, S W CHARLES DAERO-77-6-037

UNCLASSIFIED

NL

1 OF 1
ADA
065694



LEVEL II

12

The Production of Stable Ferromagnetic Liquids for Energy Conversion

1st Annual Report

by

Mr. S. R. Hoon

Dr. J. Popplewell

Dr. S. W. Charles

November 1978

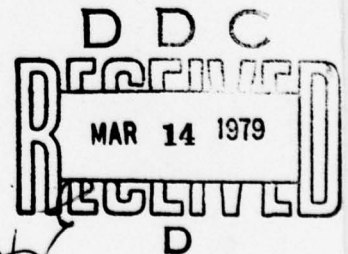
DDC FILE COPY

European Research Office,
United States Army
London W1, England

Agreement No. DAERO-77-G-37

School of Physical and Molecular Sciences,
University College of North Wales,
Bangor, Gwynedd, U.K.

Approved for public release; distribution unlimited.



79 03 08 003

AD A0 65694

UNCLASSIFIED

SECURITY CLASSIFICATION OF THIS PAGE (When Data Entered)

REPORT DOCUMENTATION PAGE		READ INSTRUCTIONS BEFORE COMPLETING FORM
1. REPORT NUMBER	2. GOVT ACCESSION NO.	3. RECIPIENT'S CATALOG NUMBER
4. TITLE (and Subtitle) THE PRODUCTION OF STABLE FERROMAGNETIC LIQUIDS FOR ENERGY CONVERSION.		5. TYPE OF REPORT & PERIOD COVERED ANNUAL REPORT, no. 1, MAY 77 - NOV 78
6. AUTHOR(s) MR. S. B. HOON, DR. J. POPPLEWELL DR. S. W. CHARLES		7. PERFORMING ORG. REPORT NUMBER
8. CONTRACT OR GRANT NUMBER(s) DAERD-77-G-037		9. PROGRAM ELEMENT, PROJECT, TASK AREA & WORK UNIT NUMBERS 6.11.02A-1T161102BH57- 04-00-643
10. CONTROLLING OFFICE NAME AND ADDRESS UNIVERSITY COLLEGE OF NORTH WALES BANGOR WALES, U.K.		11. REPORT DATE NOVEMBER 1978
12. CONTROLLING OFFICE NAME AND ADDRESS U.S. ARMY R&S GROUP (EUR) BOX 65 FPO NY 09510		13. NUMBER OF PAGES 57
14. MONITORING AGENCY NAME & ADDRESS (if different from Controlling Office) 12 59 p1		15. SECURITY CLASS. (of this report) UNCLAS
16. DISTRIBUTION STATEMENT (of this Report) APPROVED FOR PUBLIC RELEASE DISTRIBUTION UNLIMITED		15a. DECLASSIFICATION/DOWNGRADING SCHEDULE
17. DISTRIBUTION STATEMENT (of the abstract entered in Block 20, if different from Report)		
18. SUPPLEMENTARY NOTES		
19. KEY WORDS (Continue on reverse side if necessary and identify by block number) (U) FERROFLUIDS (U) SUSPENSIONS OF METALS (U) ENERGY CONVERSION		
20. ABSTRACT (Continue on reverse side if necessary and identify by block number) SEE OVER		

DD FORM 1473
1 JAN 73

EDITION OF 1 NOV 63 IS OBSOLETE

UNCLASSIFIED

SECURITY CLASSIFICATION OF THIS PAGE (When Data Entered)

409 165

UNCLASSIFIED

SECURITY CLASSIFICATION OF THIS PAGE (When Data Entered)

The aim of this research work has been to characterise the properties of suspensions of small single domain iron particles in mercury. These suspensions, or ferromagnetic liquids, have been stabilised against diffusional growth by tin and sodium additives. That the tin and sodium associate themselves with the iron particles to form coatings is strikingly shown in this report by resistivity and latent heat of melting experiments.

Settling experiments in a gravitational field indicate that in some of the fluids the iron particles aggregate to form clusters or loose flocs. These aggregates can contain as many as 10^5 iron particles. It appears, however, that the particles within the aggregates do not grow by diffusion if they are stabilized by tin and sodium coatings. This is demonstrated by magnetic data which shows that the particles retain their discrete single domain magnetic properties. Magnetic data is presented which demonstrates the importance of nearest neighbour magnetic interactions. The previously unexplained magnetic field gradient instability is also ascribed to the existence of large aggregates.

The existence of aggregates is further corroborated by viscosity, and time dependent magnetisation measurements at room temperature. A transition from a liquid to a paste-like viscosity is observed when the fluids are magnetically concentrated. The concentrated fluids behave as 'Bingham bodies'. This viscosity behaviour is also consistent with the existence of aggregates. The high, paste-like viscosity of concentrated fluids is almost wholly attributable to large quantities of mercury trapped within the aggregate structure.

That particle aggregation in fluids occurs at room temperature demonstrates that there exists in the total particle-particle interaction energy, a minimum of greater depth than kT at some finite particle separation. The total particle-particle interaction energy includes magnetic, van der Waals' and electronic charge layer terms.

Further studies are in progress to evaluate the stability of antimony coated particles, as Luborsky (15) reports that antimony has been found useful in limiting diffusional growth up to the boiling point of mercury.

The results in this report indicate that although stability of mercury based ferromagnetic liquids can be much improved by tin and sodium additives, van der Waals' forces are still responsible for the aggregation which gives rise to the undesirable high viscosities. Future work will be centred around the elimination or reduction of these attractive forces. This would thus ensure the long term stability of the fluids. It is believed that certain particle coatings will reduce the attractive van der Waals' forces.

UNCLASSIFIED

TABLE OF CONTENTS

	<u>Summary</u>	1
1.	<u>Introduction</u>	2
2.	Applications of Metallic Ferromagnetic Liquids	3
3.	Essential Properties of a Metallic Ferromagnetic Liquid	..	5
	(a) Magnetic properties	5
	(b) Ferromagnetic liquid viscosity	5
	(c) Short term stability in metallic systems	6
	(d) van der Waals' forces and aggregation	7
	(e) Diffusional growth	9
	(f) Stability in magnetic fields	9
4.	<u>Experimental</u>	12
	(a) Sample preparation	12
	(b) Magnetic measurements	12
	(c) Resistivity measurements	12
	(d) Viscosity measurements	12
	(e) Latent heats of fusion	12
5.	<u>Results and Discussion</u>	14
	(a) The magnetisation curve	14
	(b) Magnetic interactions	14
6.	<u>Time Dependent Magnetisation</u>	19
7.	<u>Gravitational Settling</u>	22
8.	<u>The Resistivity of Iron Particles in Mercury Liquids</u>	..	27
9.	<u>Viscosity Measurements</u>	38
10.	<u>Phase Changes at the Melting Point</u>	45
11.	<u>Concluding Remarks</u>	49
12.	<u>Future Work</u>	51
	<u>References</u>	52
	Publications Arising from Work Sponsored by the U.S. Army	53

List of Figures

<u>Figure</u>	<u>Caption</u>
2.1	Schematic energy conversion system
3.1	Tin stabilisation of iron particles in mercury
3.2	Sodium stabilisation of tin-coated iron particles in mercury
5.1	The effect of the demagnetisation loops
5.2	The effect of iron particle concentration upon the magnetisation curve at 77K
5.3	Change in coercive force with particle diameter of spherical iron particles as measured at 77K (after Luborsky ¹¹)
6.1	Time dependent magnetisation data at room temperature after a reduction in the applied field
7.1.1	The variation in the saturation magnetisation for a column of tin-coated iron particles left to stand for 9 months
7.1.2	The coercivity at 77K of the samples whose magnetisation is given in (7.1.1)
7.1.3	The magnetic diameters inferred from 7.1.2
7.2	The relative iron particle concentration in a 15 cm column of mercury as a function of height and time
8.1	The resistivity of tin-mercury and a 0.1 wt% tin-coated iron fluid after excess tin has been added
8.2	The variation in resistivity of an iron particle in mercury fluid upon the addition of tin
8.3	The variation in the resistivity for uncoated and tin-coated iron particles as the particle concentrations is increased
8.4	The time dependent variation in the resistivity observed for tin-coated iron particles when excess tin is added
8.5	The time dependent variation in the resistivity of a tin-coated iron particle fluid to which sodium has been added.
8.6	The variation in the resistivity of an iron particle fluid with iron concentration before and after exposure to a magnetic field gradient.
8.7	The variation in the resistivity of a tin-coated iron particle fluid and pure mercury between 77 and 300 K
8.8	The difference in the resistivities of tin-coated iron particles in mercury and pure mercury between 77 and 300 K.

- 9.1 The variation in the viscosity of an iron particle fluid as a function of iron concentration, at specific shear rates
- 9.2 Shear thinning behaviour for two iron particle in mercury fluids
- 9.3 'Bingham fluid' behaviour for a 1.157 wt % iron particle in mercury fluid
- 9.4 The limited validity of the equations (3.2) and (3.3) in explaining the observed viscosity of iron particles in mercury
- 10.1 The line shapes, for various mercury based samples, produced by the D.S.C. as the samples are melted
- 10.2 The ratio of the premelting heat to total heat of transition as a function of iron and tin concentration
- 10.3 The total heats of transition as a function of iron and tin concentration.

EXCESSION	
BY	Write Section <input checked="" type="checkbox"/>
DD	Diff Section <input type="checkbox"/>
REPRODUCED	<input type="checkbox"/>
IDENTIFICATION	
BY	
DISTRIBUTION/AVAILABILITY CODES	
Dist.	AVAIL. and/or SPECIAL
A	

DDC
RECEIVED
MAR 14 1979
D

Summary

The aim of this research work has been to characterise the properties of suspensions of small single domain iron particles in mercury. These suspensions, or ferromagnetic liquids, have been stabilised against diffusional growth by tin and sodium additives. That the tin and sodium associate themselves with the iron particles to form coatings is strikingly shown in this report by resistivity and latent heat of melting experiments.

Settling experiments in a gravitational field indicate that in some of the fluids the iron particles aggregate to form clusters or loose flocs. These aggregates can contain as many as 10^5 iron particles. It appears, however, that the particles within the aggregates do not grow by diffusion if they are stabilized by tin and sodium coatings. This is demonstrated by magnetic data which shows that the particles retain their discrete single domain magnetic properties. Magnetic data is presented which demonstrates the importance of nearest neighbour magnetic interactions. The previously unexplained magnetic field gradient instability is also ascribed to the existence of large aggregates. The existence of aggregates is further corroborated by viscosity, and time dependent magnetisation measurements at room temperature. A transition from a liquid to a paste-like viscosity is observed when the fluids are magnetically concentrated. The concentrated fluids behave as 'Bingham bodies'. This viscosity behaviour is also consistent with the existence of aggregates. The high, paste-like viscosity of concentrated fluids is almost wholly attributable to large quantities of mercury trapped within the aggregate structure. That particle aggregation in fluids occurs at room temperature demonstrates that there exists in the total particle-particle interaction energy, a minimum of greater depth than kT at some finite particle separation. The total particle-particle interaction energy includes magnetic, van der Waals' and electronic charge layer terms.

Further studies are in progress to evaluate the stability of antimony coated particles, as Luborsky (15) reports that antimony has been found useful in limiting diffusional growth up to the boiling point of mercury.

The results in this report indicate that although stability of mercury based ferromagnetic liquids can be much improved by tin and sodium additives, van der Waals' forces are still responsible for the aggregation which gives rise to the undesirable high viscosities. Future work will be centred around the elimination or reduction of these attractive forces. This would thus ensure the long term stability of the fluids. It is believed that certain particle coatings will reduce the attractive van der Waals' forces.

1. INTRODUCTION

Ferromagnetic liquids consist of suspensions of small, single domain ferromagnetic particles dispersed in a liquid carrier. The particles are made small to reduce magnetic interactions and are coated with a dispersant to prevent aggregation through van der Waal's forces. It is also a necessary requirement for most applications that the particles remain in suspension in both magnetic and gravitational field gradients. This criterion for stability is readily met by those ferromagnetic liquids, identified by the term ferrofluids, produced commercially by Ferrofluidics Corp. Such ferrofluids consist of Fe_3O_4 particles of 100-200 Å diameter, dispersed in a hydrocarbon or diester carrier. Ferrofluids using water or silicone oil as the carrier fluid are more difficult to prepare and their stability is often unpredictable.

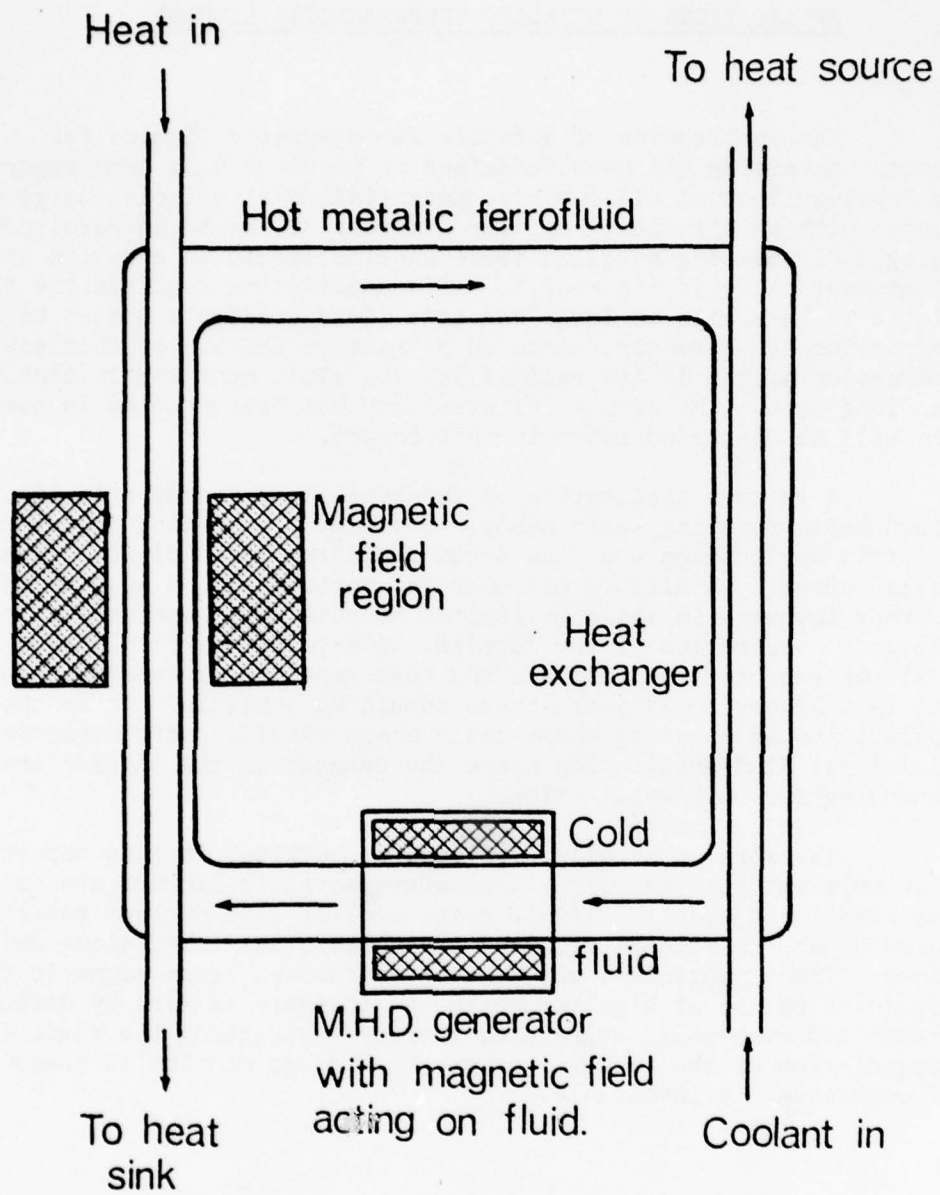
Ferromagnetic liquids containing ferromagnetic metal particles of iron or cobalt would be magnetically stronger than ferrofluids containing ferrite particles since the saturation magnetisation of these elements is appreciably greater ($I_s(\text{Fe}_3\text{O}_4) = 480 \text{ emu/cc}$. $I_s(\text{Fe}) = 1707 \text{ emu/cc}$). Their use in devices would, therefore, be expected to be more extensive. Moreover, if the carrier is a liquid metal such as mercury the high thermal and electrical conductivity makes possible other uses of the fluids, e.g. in switches and in energy conversion systems. Ferromagnetic liquids of this type containing iron particles in mercury are the subject of this report.

2. APPLICATIONS OF METALLIC FERROMAGNETIC LIQUIDS

The application of metallic ferromagnetic liquids for energy conversion has been described in previous U.S. Army reports and by Popplewell et al (1) (1976). Essentially, a reliable energy conversion system with an efficiency of approximately 30% could be developed using a circulating metallic ferromagnetic liquid in a device shown diagrammatically in figure 2.1. This application requires the ferromagnetic liquid to be stable in large magnetic field gradients and at high temperatures. Moreover, since an attractive feature of this energy conversion system is its reliability the fluid must remain stable over the long term. The problem of stability has been studied in some detail and will be discussed later in this report.

A further application of the metallic ferromagnetic liquid would be in rotating shaft seals. Normally the sealing ferrofluid recommended for this application would be a 400 G diester based fluid. Although seals currently available may operate continuously at 60,000 r.p.m. further increase in speed is limited because heat generated in the seal produces evaporation of the carrier. A metallic carrier, however, would be expected to dissipate the heat generated more effectively and thus higher rotational speeds should be possible. It is the application in rotating shaft seals where metallic ferromagnetic liquids will first find application since the demands on the liquids are less demanding for this application.

The work on metallic systems, as outlined in this report, is also relevant to other situations where metallic liquids are used. It has been found that the liquid metal coolant in a nuclear reactor acquires ferromagnetic particles from the stainless steel tubes along which it flows. These particles, which may pass through large magnetic field gradients and be at high temperatures, increase in size by diffusional growth and eventually aggregate, thereby restricting the fluid flow. An appreciation of the kinetics of growth and aggregation in these circumstances is invaluable.



Figure(2.1). Schematic energy conversion system

3. ESSENTIAL PROPERTIES OF A METALLIC FERROMAGNETIC LIQUID

(a) Magnetic properties

It is desirable to produce ferromagnetic liquids with a high saturation magnetisation and a large initial susceptibility. This is best achieved by selecting iron or cobalt (I_S (Fe) = 1707 emu/cc, I_S (Co) = 1400 emu/cc) as the ferromagnetic particle component. The particles must be made small, ~ 45 Å diameter, in order to prevent aggregation due to magnetostatic interactions. The particle concentration in the carrier must also be large if the saturation magnetisation of the liquid is to be large. Commercial ferrofluids containing Fe_3O_4 particles normally have a magnetisation ($M_S = 4\pi I_S$) of 100 - 400 G. Such magnetisations correspond to particle concentrations of $\sim 10^{17}$ /cc or some 10 volume %. The maximum particle concentration and hence the maximum magnetisation is limited by the final viscosity of the ferrofluid. This is a particularly important consideration in the preparation of strong metallic ferromagnetic liquids. Although metallic systems can be prepared with $M_S \sim 400$ G the magnetic particle concentration is only 2-3% by volume. Above this value the ferromagnetic liquid acquires a high and unacceptable viscosity. Clearly, in order to improve the fluid magnetisation it is necessary to increase the particle content whilst maintaining a low viscosity. Hence the study of the factors determining the high viscosities in fluids of low particle concentrations, as given in this report, is considered vital to any further development of metallic ferromagnetic liquids.

(b) Ferromagnetic Liquid Viscosity

Commercial ferrofluids of 100 - 200 G saturation magnetisation have viscosities of a few centipoise. A concentrated fluid of 600 G may have a viscosity of 200 cp.

The Einstein equation for the ferrofluid viscosity η_f ,

$$\eta_f/\eta_o = 1 + 2.5 \phi \quad (1)$$

where η_o is the carrier viscosity and ϕ the solid fraction, may be expected to apply for low concentrations where the particle radius is small compared with the particle separation. For more concentrated systems the relation

$$\frac{\eta_f - \eta_o}{\eta_f} = 2.5 \phi - \left[\frac{2.5\phi_c - 1}{\phi_c^2} \right] \phi^2 \quad (2)$$

due to De Bruyn (2) is more appropriate. ϕ_c represents a critical concentration at which the fluid becomes solid. A value of $\phi_c = 0.74$ corresponding to hexagonal close packed spheres would seem to be a reasonable value to take for the ferrofluid system (Rosensweig et al (3) 1965). ϕ is related to the volume fraction ϵ and particle coating δ by the expression

$$\phi = \epsilon \left[1 + \frac{\delta}{r} \right]^3 \quad (3)$$

It is clear from expressions (2) and (3) that the viscosity of ferrofluids depends on the size of the surfactant coating since the physical diameter rather than the magnetic diameter is important.

It is possible that the high viscosities found in metallic systems arise partially from adsorbed mercury layers on the particles, which effectively increase the physical size in a similar manner to the dispersant coatings in non-metallic systems. Further effects arising from particle interactions may be important and are under investigation. The latter could be particularly serious in metallic systems where repulsive forces between particles, necessary to prevent particle aggregation, may be negligible.

(c) Short term stability in metallic systems

The short term stability of a ferromagnetic liquid is determined by particle interactions and the presence of magnetic or gravitational field gradients. In the simplest situation particles may aggregate under magnetic or van der Waal's forces and then settle under gravitational forces. Agglomeration through magnetic interactions may be prevented if the magnetic energy of particles in contact is less than the thermal energy transmitted to the particles through the carrier liquid. For two spherical particles, stability in the presence of magnetic interactions would occur when

$$\frac{2\mu^2}{D^3} = \frac{\pi^2 D^3 I_s^2}{18} < kT \quad (4)$$

where D is the particle diameter, I_s the saturation magnetisation at temperature T and μ the magnetic moment of a particle. Hence aggregation through magnetic interactions for iron particles with $D = 30 \text{ \AA}$ or Fe_3O_4 particles with $D = 100 \text{ \AA}$ would be insignificant at 200°C .

Aggregation may also take place through van der Waal's forces which are short range compared with the magnetic force between particles. For small distances between spherical particles this leads to an expression for the energy

$$U = -AD/24S \quad S \ll D \text{ and } S > 4\text{\AA} \quad (5)$$

and at large distances

$$U = \frac{-16}{9} A (D/2S)^6 \quad S \gg D \quad (6)$$

where D is the particle diameter, $S = X-D$, X the centre to centre

distance between particles and $A = \pi^2 n^2 \lambda$ where n is the number of atoms / cc, $\lambda = \frac{3}{4} h \nu_0 \alpha^2$, α is the polarizability and $h\nu_0$ is a characteristic ionisation energy. Aggregation through van der Waal's forces is prevented in ferrofluids by coating the particles with a dispersant such as oleic acid, a long chain polar molecule of length $\sim 11A$, which produces an entropic repulsion between particles.

The prevention of aggregation whether due to magnetic or van der Waal's interactions is difficult since a particle size distribution must always be considered and large particles which seed the aggregation will always be present. In commercial ferrofluids the problem is minimised by removing the large particles by centrifuging. This improves the stability significantly. In metallic systems the larger particles may be removed by magnetic separation provided the particle concentration and size distribution is such that aggregation does not occur before or during separation. These conditions are difficult to achieve in metallic systems. Aggregation due to van der Waal's forces (in metallic systems) cannot be prevented using entropic repulsion at present since there are no known metal-compatible dispersants equivalent to oleic acid. This is the main obstacle to the preparation of stable metallic ferromagnetic liquids.

(d) Van der Waals' forces and aggregation

The problem of aggregation (coagulation) in colloidal systems was first investigated by Smolowski (4). He considered the particles to have no long range attraction for one another and to stick together when they come within a critical interaction distance $2R$. The total number of aggregates/cc at time t was shown to be given by

$$n = n_0 \left[1 + 4 \pi \Phi R n_0 t \right]^{-1} \quad (7)$$

where n_0 is the number of aggregates/cc at $t = 0$ and Φ is the diffusion coefficient. Since Φ is inversely proportional to R , n is independent of particle size.

If D is given by the Stokes-Einstein relation equation (7) may be rewritten

$$n = n_0 \left[1 + \frac{t}{\theta} \right]^{-1} \quad (8)$$

$$\text{where } \theta = \frac{1}{4 \pi \Phi R n_0} = \frac{3\eta}{4 k T n_0} \quad (9)$$

For a 1 wt % iron in mercury fluid with 40 Å diameter particles $n_0 \sim 10^{17}/\text{cc}$. With $\eta = 1 \text{ p}$, as observed for a 1 wt % fluid, $\theta \sim 10^{-4}$ secs at room temperature, i.e. the number of aggregates is reduced by a half in 10^{-4} secs. θ is a measure of the coagulation time in the absence of long range interactions. In the presence of interactions an effective coagulation time $\theta^* = q \theta$ may be defined where

$$q = 2R \int_{2R}^{\infty} r^2 \exp\left[\frac{W}{kT}\right] dr \quad (10)$$

where W denotes the interaction energy which may be positive or negative depending on whether the interaction is attractive or repulsive. A value of q equal to 0.66 has been calculated by Hoon (5) for a van der Waals' attractive interaction in the iron-mercury system. Since $\theta \sim \theta^*$ aggregation of iron particles in mercury fluids would take place quickly in the absence of any repulsive interaction. Furthermore, this aggregation causes settlement to take place. However, $m^* gh \ll kT$ is the condition for stability in a gravitational field where $m^* = \frac{4}{3} \pi R^3 \rho^*$ (11) and $\rho^* = \rho_{Hg} - \rho_{Fe}$ is the effective density of the particles in mercury. Thus for an aggregate containing x spherical iron particles of radius R a distance of 1 cm below the mercury surface, the condition for sedimentation is given by

$$m^* gh \sim \frac{4}{3} \pi R^3 \rho^* x gh > kT \quad (12)$$

Setting R to 20 Å predicts $x > 10^2$ particles. Equation (8) shows that this aggregation takes place in a time $t \sim 10^{-2}$ secs. Thus settling takes place rapidly in the absence of repulsive particle/particle interactions. Moreover, since settling increases the local particle density, aggregation may be expected to increase more rapidly as settling takes place.

The prevention of aggregation due to van der Waals' forces is difficult. Though these forces may be expected to have a shorter range in metallic systems it is still present and would probably lead to aggregation. The use of particle coatings to reduce this interaction has been considered by Hoon et al (6). In this case the possibility of coatings forming charged surface layers through charge transfer at the interface between the particle surface and the carrier is considered. The situation thus existing at the particle surface is analogous to the charged double layers in colloids in non-metallic systems. Hoon et al (6) were able to show that the spacial extent of the charge depended on the difference in Fermi energy between carrier and particle and the magnitude of the charge transfer on the difference of the work functions of the two metals. Thus sodium with a work function very different from that of iron or mercury would be an appropriate coating material for the particles. Calculations show that though charge transfer should indeed take place the assumptions in the theory make it uncertain whether it would be sufficient to provide the necessary repulsion between particles to make the system stable.

(e) Diffusional Growth

In metallic systems ferromagnetic liquids may become unstable if particle growth takes place. This arises in a metallic carrier if the particles are not of one size. The larger particles will grow at the expense of the smaller particles through diffusion of atoms from the surfaces of small particles where the surface energy is large to the surfaces of large particles where the surface energy is low. The surface of the iron particles may be protected with coatings of tin or sodium and in this way diffusional growth may be prevented as shown in figures (3.1) and (3.2). The experiments relating to diffusional growth have been described by Windle et al (7) and Hoon et al (6). Their results are consistent with the theory of Greenwood (8) who predicts that the particle growth rate is a maximum for particles with a radius (a_{2m}) twice that of the mean and that $a_{2m}^3 \propto t$.

As can be seen from figure 3.1 for iron particles aged in mercury, particle growth is evident in the long term and stability is not obtained. However, as shown in figure 3.2, long term growth is prevented for particles initially coated with tin and subsequently coated with sodium. It was uncertain, in the early experiments described by Hoon et al (6) whether the sodium actually formed a particle coating. However, recent measurements on the resistivity would suggest that this is the case. Such measurements are reported in the results of section 3.

(f) Stability in Magnetic Fields

The stability of a ferromagnetic liquid depends on the magnitude of the magnetic field gradient acting on it. The liquid would be considered unstable if the ferromagnetic particles separated out from the carrier. Since the ferromagnetic particles experience a force

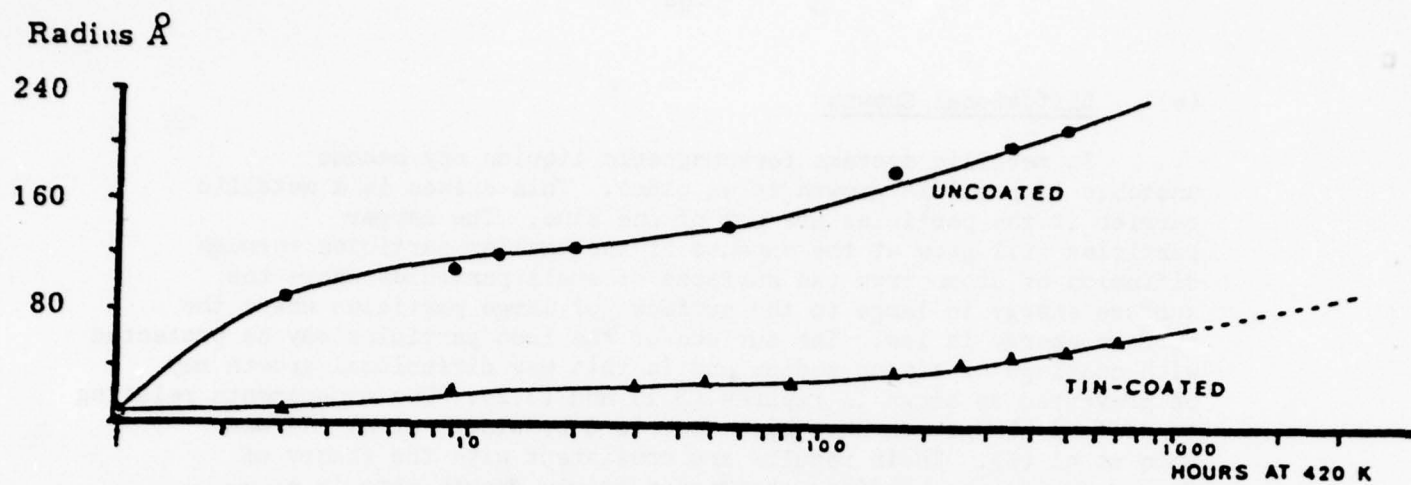
$$\underline{F}_m = \frac{(\underline{M} \cdot \underline{\nabla}) \underline{H}}{4 \pi} \frac{\pi D^3}{6} \quad (13)$$

in a field gradient $\underline{\nabla} \cdot \underline{H}$ the particles reach a terminal velocity \underline{u} when the magnetic \underline{F}_m and viscous \underline{F}_s forces are equal. \underline{F}_s is given in terms of \underline{u} and the viscosity η_o by

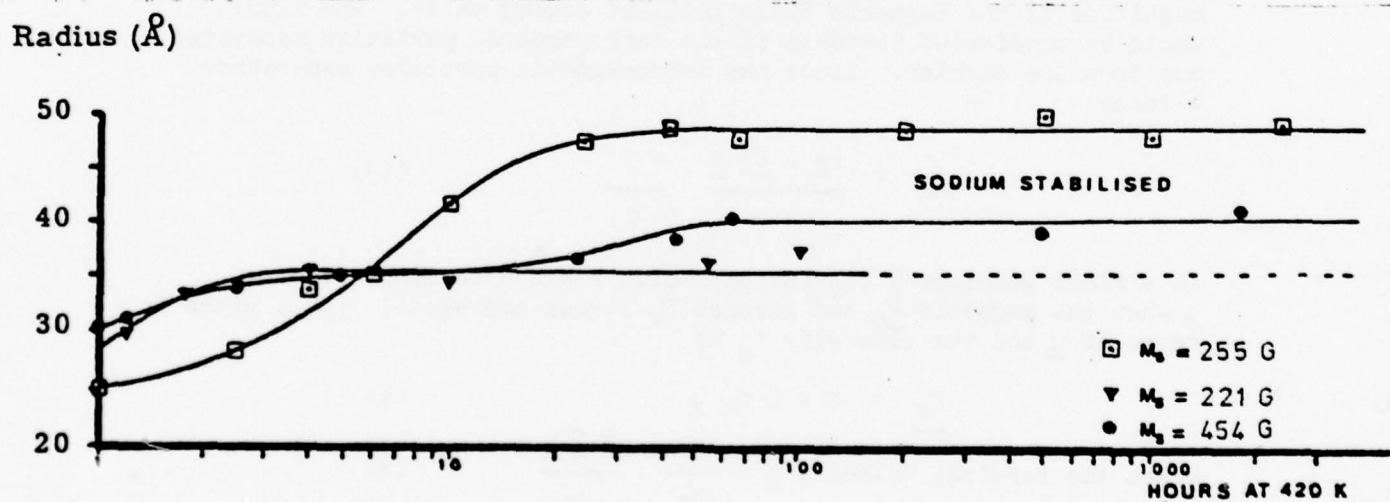
$$\underline{F}_s = 3 \pi D \eta_o \underline{u} \quad (14)$$

$$\text{Hence the terminal velocity } \underline{u} = \frac{D^2}{18\eta_o} \cdot \frac{\underline{M} \cdot \underline{\nabla} \cdot \underline{H}}{4\pi} \quad (15)$$

Equating the particle flux $n\underline{u}$ (n = the number of particles/cc) with the flux due to diffusion $\nabla n kT / 3\pi \eta_o D$ (as given by the Einstein relation), gives a steady state condition when



Figure(3.1) Tin stabilisation of iron particles in mercury



Figure(3.2) Sodium stabilisation of tin-coated iron particles in mercury

$$D^3 = 24 \left| \frac{\nabla n}{n} \right| \frac{kT}{\underline{M} \cdot \underline{\nabla} \cdot \underline{M}} \quad (16)$$

A criterion of stability, $\frac{\nabla n}{n} = 1 \text{ cm}^{-1}$ is usually adopted. This represents a 100% change in concentration for each centimetre. Hence iron particles of $D \sim 15 \text{ \AA}$ dispersed in mercury would be expected to be 'stable' in a field gradient $\underline{\nabla} \cdot \underline{H} \sim 10^4 \text{ Oe/cm}$. An overriding consideration, however, would be the time τ to reach the steady state condition. Indeed it can be shown that in a field gradient of 10^4 Oe/cm it would take one hour to reach steady state conditions. When this time is large compared with the time spent by the fluid in the field, as might be the case for the energy conversion system described in figure 1, the fluid can be described as 'stable' for all practical purposes. Stability as defined in this way thus depends on the calculation of u in equation (15).

4. EXPERIMENTAL

(a) Sample Preparation

Ferromagnetic liquids containing iron particles were prepared by electrodepositing iron on to a mercury - tin amalgam cathode. The anode was made of platinum and the electrolyte was an aqueous solution of ferrous chloride. Magnetic agitation by an alternating field of 200 G was found to be necessary in addition to mechanical stirring of the mercury amalgam surface in order to prevent particle dendrites forming on the surface of the cathode. Ferromagnetic liquids with a saturation magnetisation of up to 400 G, corresponding to ~ 2 wt % iron were prepared by this method.

The iron particles were coated with tin to prevent diffusional growth as outlined in section 1(e) by adding 0.7 wt % tin to the mercury prior to deposition. However, sodium which was found to enhance stability by forming a second coating could only be added after the preparation because of the reaction of sodium with the aqueous electrolyte. About 2 wt % of sodium was added by mixing stock sodium amalgam of known composition with the iron-mercury amalgam.

(b) Magnetic Measurements

The magnetisation $M = 4 \pi I$ was measured in fields up to 9K Oe at room temperature and 77K with a vibrating sample magnetometer. Measurements were thus made in both liquid and solid samples.

In general, the samples were superparamagnetic in the liquid state but possessed a remanence and coercivity in the solid. These measurements were useful in evaluating particle sizes and the size distribution.

(c) Resistivity Measurements

The resistivity of a number of metallic samples was measured at room temperature and temperatures down to 77K using a standard four probe method with current reversal. Only in those fluids containing sodium was difficulty encountered. These measurements are less reliable because of the reactivity of sodium with atmospheric water which caused the formation of bubbles in the cell. Resistances could be measured accurately to $\pm 10^{-6} \Omega$.

(d) Viscosity Measurements

The viscosity was measured at room temperature for different shear stresses and shear rates using a specially designed Poiseuille flow viscometer. The quantity of ferromagnetic liquid required for this experiment was of the order of 8 cm³. The use of various other methods of measuring the viscosity were attempted but the high surface tension and density of mercury precluded the use of most of these methods. Viscosity measurements were made in the range $10^{-2} \text{ p} < \eta < 10^5 \text{ p}$ ie a range reflecting the transition from

the viscosity of pure mercury to that of a self supporting paste.

(e) Latent heats of fusion

Latent heats of fusion were obtained using a commercial Perkin-Elmer differential scanning calorimeter with a sensitivity of $\sim 5 \text{ m cal K}^{-1} \text{ s}^{-1}$ using scan rates of 0.5 K min^{-1} to 8 K min^{-1} in the range 180K to 300K. A sample volume of $\sim 15 \times 10^{-3} \text{ cm}^3$ was required and yielded latent heats of fusion to a reproducibility of $\sim 5\%$. Because of the limitations of the dewar it was necessary to slow quench the samples from room temperature to below 230 K (their approximate freezing point) at a rate of $\sim 5 \text{ K min}^{-1}$. It was possible to detect the presence of $\sim 0.01 \text{ wt } \% \text{ Sn}$ in solution by examining the line-shape which was important when determining the spatial location of tin.

5. RESULTS AND DISCUSSION

(a) The Magnetisation Curve

The magnetisation curves for ferromagnetic liquids containing iron particles in mercury have been determined at 77K and room temperature. The iron concentration is determined from saturation values and the particle sizes and size distribution from remanence and coercivity data at 77K. The latter measurements have been found to be invaluable since techniques determining particle sizes from electron microscopy have required the removal of particles from the fluid and this produces unrepresentative samples. The analysis of the magnetisation curve at 77K in terms of the particle size distribution has been discussed fully in previous reports and by Chantrell et al (9).

(b) Magnetic Interactions

The effect of particle interactions on the magnetisation curve is important in the analysis of magnetisation measurements. If the particles form chains, rings or clusters the coercivity may be expected to be different from that of a system of isolated particles. The particle concentration would also be expected to be important and the overall sample shape may require the inclusion of a demagnetising factor to the applied field.

Figure (5.1) shows magnetic measurements made on a fluid containing tin-coated 45 Å diameter particles in mercury at room temperature. The fluid is superparamagnetic and there is no remanence or coercivity. The measurements are shown to be independent of the sample shape and the inclusion of a demagnetising factor would not, therefore, appear to be necessary. Since Kondorskii (10) also rules out the inclusion of a Lorentz field correction on theoretical grounds, particle interactions from nearest neighbours would seem important in determining the form of the magnetisation curve, particularly in concentrated samples.

Figure (5.2) shows a series of magnetisation curves at 77K. Various concentrations are considered in the range 10^{15} - 10^{17} particles/cc. The particle size distribution is the same for each sample. It is noted that the remanence and coercivity decreases in value by some 20% in the magnetisation range .06 to 0.4 emu/g but there is a negligible change in the range 0.4 to 3.32 emu/g; that is above 0.2 wt % iron. The samples used for the measurements shown in fig (5.2) are obtained after the sample has been frozen in a field of 35 Oe, a field which might not be expected to produce significant particle chaining in the liquid state. If chaining did take place the coercivity as measured in the solid state at 77K would be expected to be greater than for a system of isolated particles. The observed reduction in coercivity as the particle concentration is increased cannot, therefore, be attributed to simple chain formation. Furthermore, a fluid cooled in a strong field at 10 k Oe possesses the same coercivity as a sample cooled in zero field. The reduction in coercivity with concentration is thus more likely to be associated with the formation of ring type clusters rather than chains.

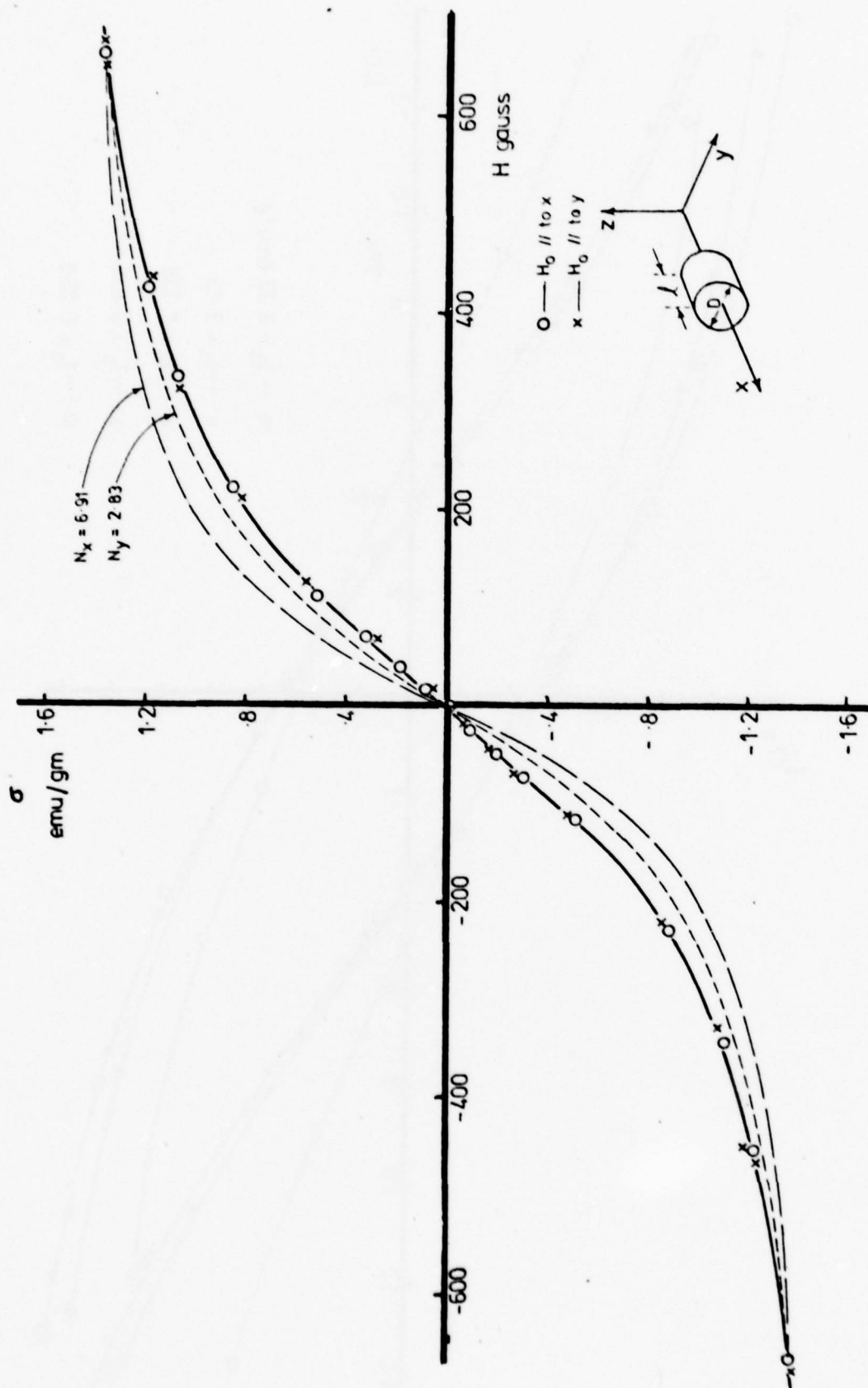


Figure (5.1) The superposition of the experimental points for H_{\perp} and H_{\parallel} to the samples x direction without the need for a demagnetising field correction.

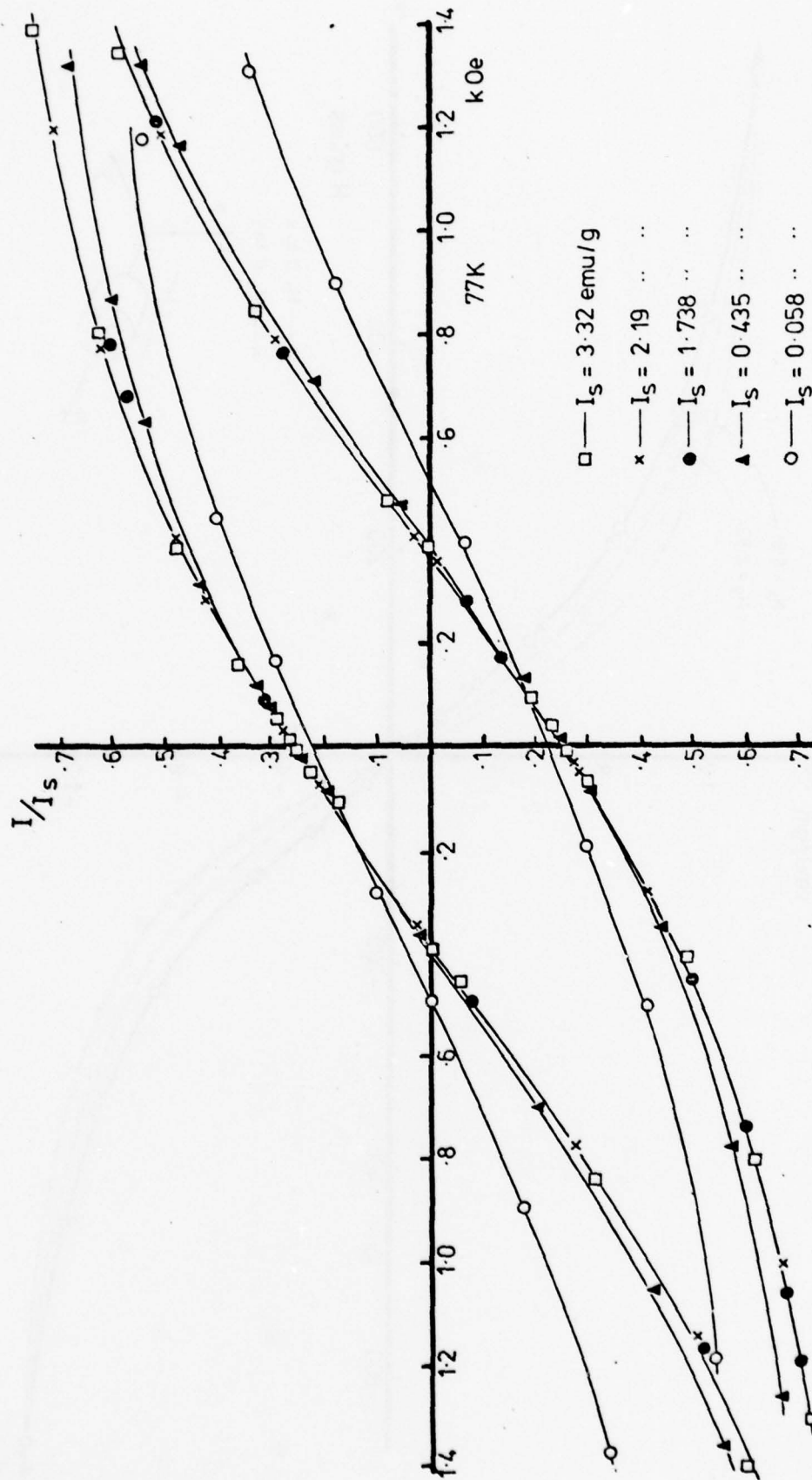
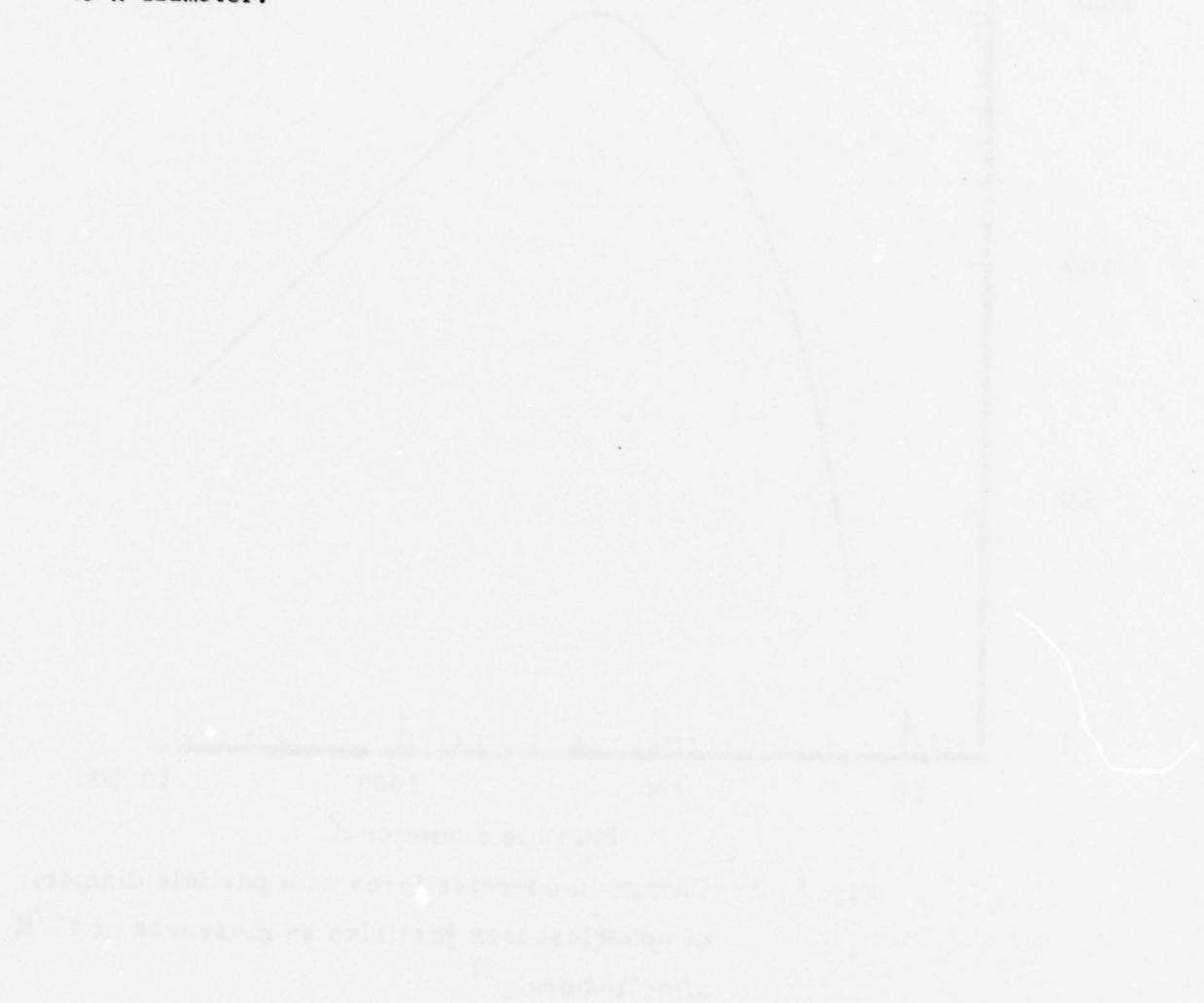


Figure (5.2) shows the effect of iron particle concentration upon the magnetisation curve at 77K.

Finally, it should be pointed out that the change of 20% in the coercivity with increased concentration would not seriously change estimates of particle size as determined from the Luborsky (11) coercivity-size plot figure (5.3) for particles of approximately 45 A diameter.



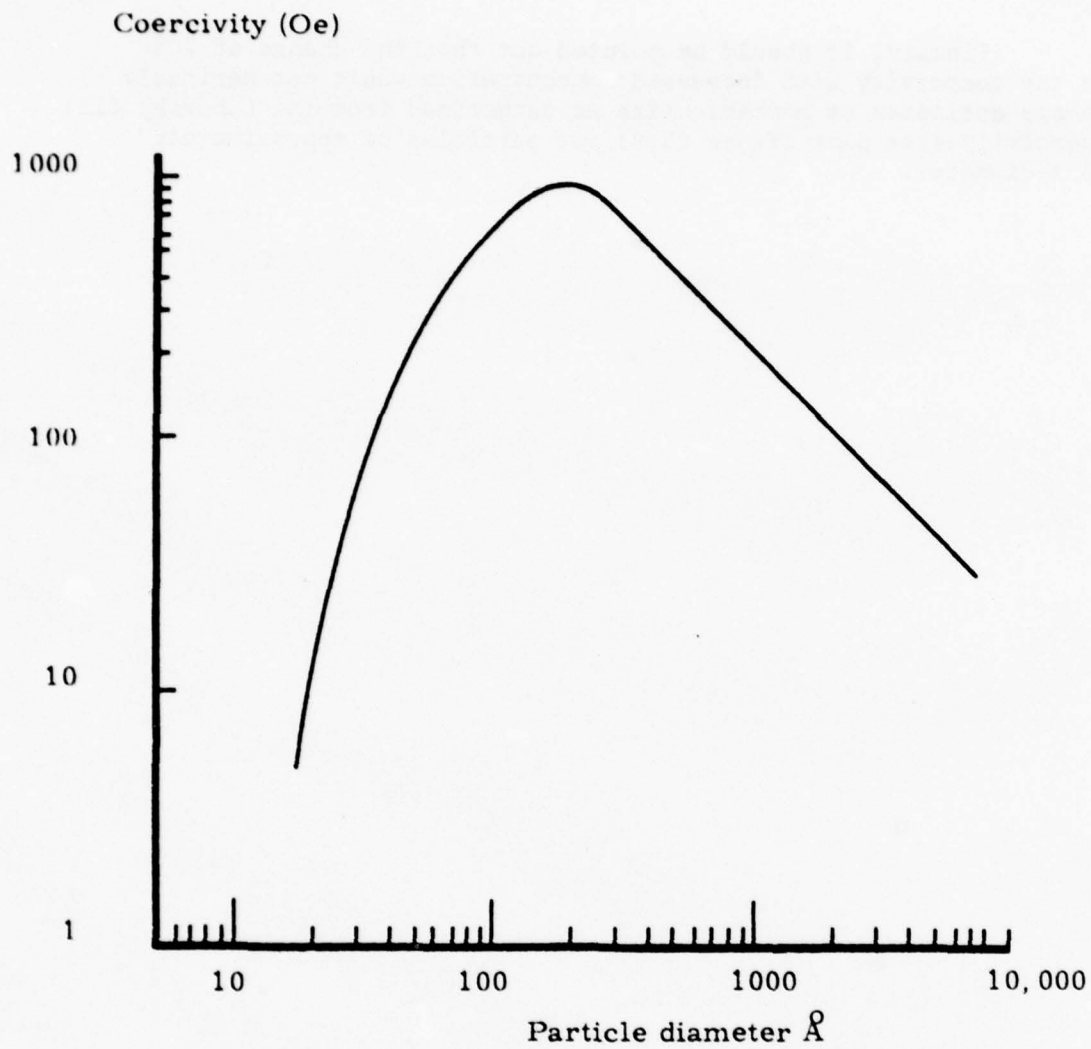


Fig. 5. 3: Change in coercive force with particle diameter of spherical iron particles as measured at 77°K , after Luborsky¹¹.

6. TIME DEPENDENT MAGNETISATION

Figure 6.1 shows time dependent magnetisation measurements at room temperature for 1.47 emu/g and 0.49 emu/g tin coated iron particles in mercury. Both these fluids have viscosities similar to that of mercury. In each case the applied magnetic field has been reduced quickly from the value H_1 to the value of H_2 (these values being indicated in figure 6.1). The observed characteristic times for the magnetisation to decay are ~ 30 secs. Such long time constants can only be due to large particles or aggregates whose moments are blocked within the particles, such that the magnetic moment can only relax by bulk particle rotation. For a blocked particle the energy barrier to rotation of the magnetic vector is larger than the thermal energy kT . The magnitude of the energy barrier is determined by the anisotropy K . Where K may be considered to be the sum of the shape, crystal and interaction anisotropies. For unblocked particles the relaxation time would be $\sim 10^{-11}$ secs. This is about 10^{-2} times shorter than the characteristic time constant for Brownian relaxation of an individual 40 Å diameter particle.

Shliomis (12) has shown that the relaxation time for blocked particles in a magnetic field is given approximately by

$$\tau \sim \eta V / \mu H \quad (6.1)$$

where τ is the time for the magnetic moment to rotate through π radians, η is the carrier viscosity, V the hydrodynamic particle volume, $\mu = \frac{4}{3} \pi a^3 I'_s$ the magnetic moment, a the particle radius and H is the applied field. I'_s is the bulk material's saturation magnetisation.

Equation (6.1) can be extended to cover the case where the hydrodynamic volume is greater than the magnetic volume, i.e. the volume of the magnetic material is less than the hydrodynamic volume. Thus

$$\tau \sim \frac{6\eta}{I'_s H} (1 + \delta/a)^3 \quad (6.2)$$

where δ is the thickness of an adsorbed layer. For small particles

$$\tau_p < 48 \eta / I'_s H \quad (6.3)$$

represents the relaxation time for individual particles. For large particles of aggregates ($a > 200\text{Å}$) it is reasonable to assume $\delta/a \ll 1$ and thus the relaxation time of an aggregate τ_{agg} is given by

$$\tau_{agg} \sim 6 \eta / I'_s H \quad (6.4)$$

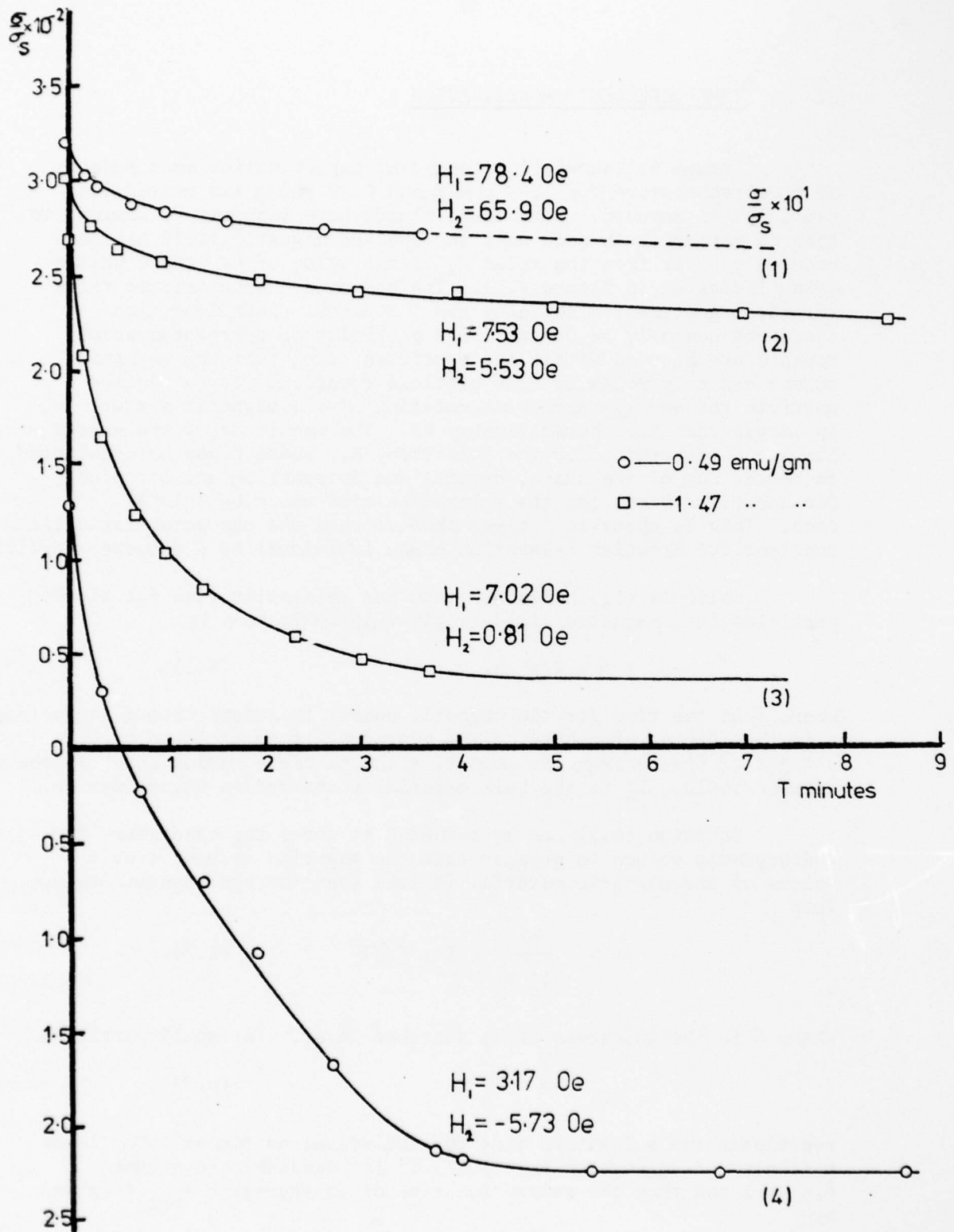


Figure (6.1) shows the time dependent magnetisation data for iron particles in mercury when the applied magnetic field is reduced from H_1 to H_2 Oe. (at room temperature)

Application of equations (6.3) and (6.4) to the curve (iv) in figure (6.1) predicts $\tau_p \sim \tau_{agg} \sim 10^{-3}$ secs, where I_s' has been taken as 1707 emu/cc and $H \sim 10$ Oe. In practice τ is observed to be ~ 30 secs.

To obtain agreement between experiment and theory it is necessary to assume that aggregates of particles form, such that their net moment is reduced by flux closure configurations. This would be consistent with the conclusions reached in section (5) to explain the reduced coercivity measurements observed for concentrated iron samples. It is possible to remove the complication that flux closure makes in interpreting the curves of figure (6.1) by considering the simpler case (iii), of that figure. This is because for curve (iii) the applied field has been effectively switched off at $t = 0$ and so the magnetisation decays only by Brownian diffusional rotation of the particles or aggregates. In this case τ is given by

$$\tau_B \sim 3 V \eta / k T \quad (6.5)$$

Let the radius of a particle $a \sim \frac{1}{2} V^{\frac{1}{3}}$ then

$$a \sim \frac{1}{2} \left[\frac{\tau k T}{3 \eta} \right]^{\frac{1}{3}} \quad (6.6)$$

Then for $\eta \sim 1p$ and $\tau \sim 30$ secs equation (6.6) yields $a \sim 10^{-4}$ cm. This value of a is in agreement with the calculated aggregate size inferred from gravitational stability experiments.

It should also be noted that equation (6.6) is not very sensitive to η , as for $\eta \sim 10^{-2}p$, $a \sim 2 \times 10^{-4}$ cm. For high viscosity fluids, paste-like in appearance, ie $\eta > 10^3 p$, equation (6.6) predicts for a $\sim 10^{-4}$ cm a value of τ of 30 hours. If a paste-like fluid is saturated in a magnetic field and then the field removed a remanence is observed which disappears in a time similar to that calculated above ie ~ 24 hours.

7. GRAVITATIONAL SETTLING

The particles in a ferromagnetic liquid are not uniformly distributed in a gravitational field. At temperature T the number of particles per unit volume at a height h is given by the Boltzmann distribution,

$$N = N_0 \exp \left[-m^*gh/kT \right]$$

where $m^* = \frac{4}{3} \pi a^3 \rho^*$, $\rho^* = \rho_{Hg} - \rho_{particle}$ and a is the particle radius.

The saturation magnetisation of the fluid is given by

$I_s = I'_s \epsilon$ where ϵ is the volume fraction of particles whose material has the bulk saturation value I'_s .
and $\epsilon = N \frac{4}{3} \pi a^3$.

Hence

$$I_s = I'_s \frac{4}{3} \pi a^3 N_0 \exp \left[-m^*gh/kT \right] \quad (7.1)$$

represents the saturation magnetisation as a function of height h for a column of single unaggregated ferromagnetic particles. In practice systems have a particle size distribution and the probability of finding a particle of volume V is related to the log normal distribution $f(y)$. Where $f(y)$ is given by

$$f(y) = \left[\exp \left(-\ln y \right)^2 / 2 \sigma^2 \right] / y \sigma \sqrt{2\pi} \quad (7.2)$$

$f(y) dy$ is the fraction of the magnetic volume having reduced diameter $y = D/D_v$ in the range y to $y+dy$. D_v is the median particle diameter of the volume distribution.

Figure (7.1.1) shows the observed variation in I_s with h when a tin coated iron fluid of ~ 2 wt % Fe was left for 9 months to come to equilibrium in a gravitational field. The theoretical curves are computed from equation (7.1) assuming the particles to be monodispersed. The deviation from such curves can be explained in terms of a particle size distribution. Larger particles will be more common the lower the value of h , and as their contribution to I_s is volume dependent, a small number can constitute the major contribution to I_s . Allowing for small departures, a monodispersed 140A diameter particle fluid would give almost identical behaviour to that shown in figure (7.1.1).

Figure (7.1.2) shows the observed coercivity of the samples used for figure (7.1.1) at 77K. From these are inferred the characteristic particle diameters, of the order of 40 A, plotted in figure (7.1.3). The discrepancy between 40A and 140A is marked. It is expected from equation (7.1) that as h increases the ratio of smaller particles to larger should increase. Thus the coercivity should decrease as observed. The particle diameters inferred from figure (7.1.3) and figure (7.1.) are in disagreement unless it is supposed that the magnetic

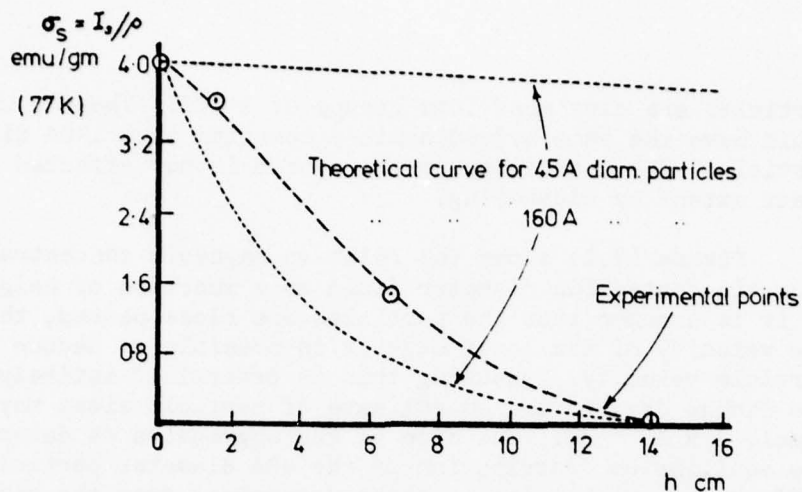


Figure (7.1.1) shows the variation in σ_s for column of tin-coated fluid left to stand for 9 months

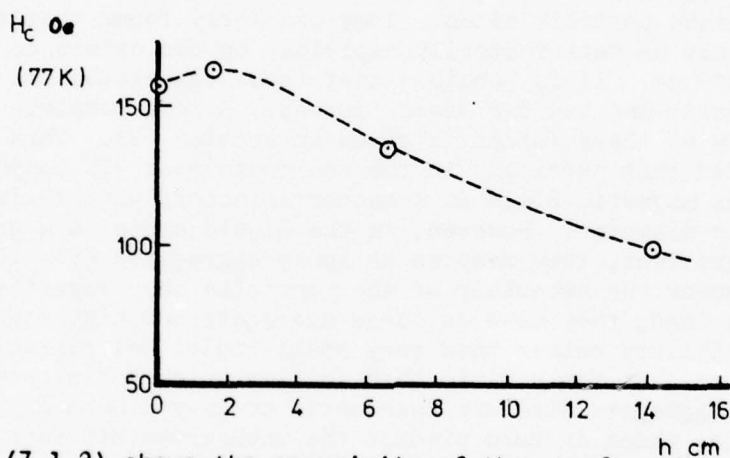


Figure (7.1.2) shows the coercivity of the samples whose magnetisation is given in (7.1.1)

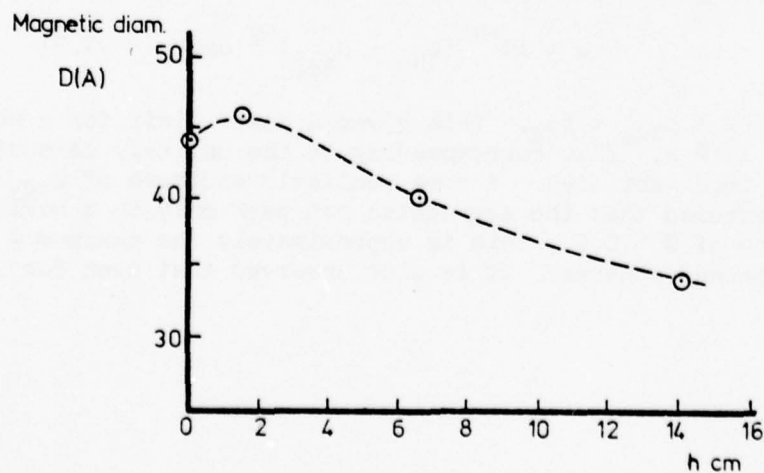


Figure (7.1.3) shows the magnetic particle diameter inferred from figure (7.1.2)

particles are clustered into groups of ~ 100 . These clusters would have the same hydrodynamic properties as a 140A diameter particle. The coercivity of the system is not affected to any great extent by clustering.

Figure (7.2) shows the relative magnetic concentration $I_S(h)/I_S$ of a tin coated 60A diameter fluid as a function of height and time t . If it is assumed that the particles are close packed, then from the velocity of the lower edge it is possible to deduce a terminal particle velocity. Assuming this is determined entirely by the Stokes drag force, an estimate of particle sizes may be made, namely 2×10^{-4} cm. The size of the aggregates as determined from the equilibrium distribution of the 40A diameter particles is markedly different from the size of those determined from the time dependent measurements for the fluid containing 60A diameter particles. This may demonstrate that the factors determining aggregation are very sensitive to particle size.

Other workers (13,14) have also used sedimentation experiments to estimate particle sizes. They similarly found that their results could only be satisfactorily explained by the existence of aggregates of $\sim 10^{-4}$ cm. It is possible that these aggregates are held together by magnetic and van der Waals' forces. A more complete discussion of the role of these forces is given in section (3). Thus it must be concluded that particles in the solid state at 77K respond to an external magnetic field in a manner in accord with their individual magnetic diameter. However, in the liquid state in a gravitational field gradient, they respond as loose aggregates of $\sim 10^{-4}$ cms. In this manner the behaviour of the particles in a magnetic field gradient is explained; they move as large aggregates of high magnetic susceptibility rather than very small individual particles. It may be argued that for a fluid that settles quickly the above estimates of the aggregate size are inaccurate as they assume high particle packing densities which in turn predict the unobserved attainment of high fluid magnetisations. It is shown here that the close packing assumption is not as limiting as it appears at first sight.

From the sedimentation experiments it follows that the aggregates radius is given by

$$a \sim 10^{-4} (\rho_{Hg} - \rho_{agg})^{-\frac{1}{2}} \text{ cm.} \quad (7.3)$$

where $\rho_{Fe} < \rho_{agg} < \rho_{Hg}$. This gives a lower limit for a when $\rho_{agg} = \rho_{Fe}$ of 4×10^{-5} A. This corresponding to the unlikely case of close packed iron particles. A more realistic estimate of ρ_{agg} can be made if it is assumed that the aggregates can pack only to a maximum volume fraction of $\phi \sim 0.5$. This is approximately the maximum ϕ for cubic packed spheres. It is also observed that even for the fluids that

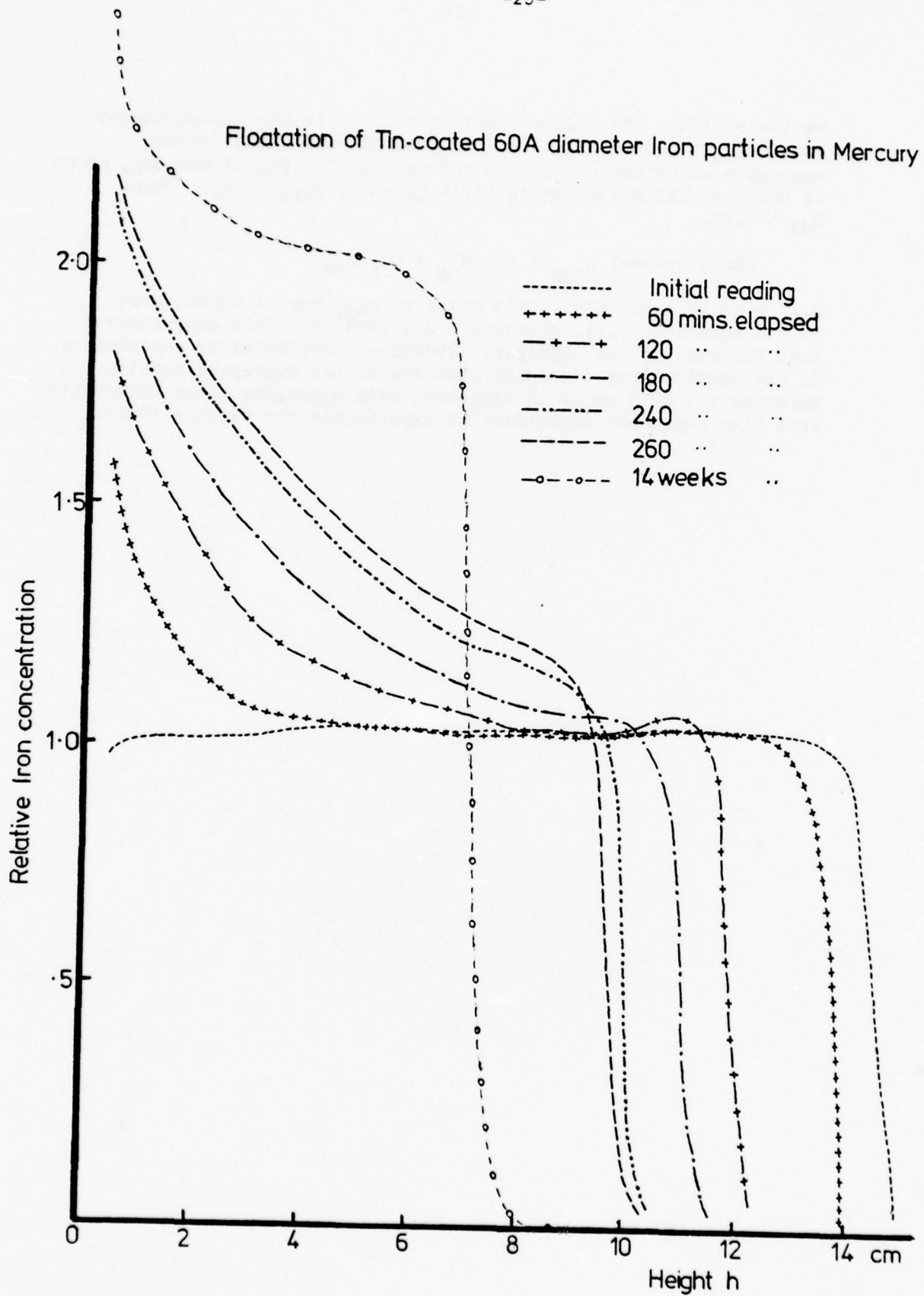


Figure (7.2) shows the relative iron particle concentration in a 15 cm column of mercury as a function of height and time.

settle rapidly, the volume fraction of iron in the system cannot exceed $\phi_{Fe} \sim 0.02$. All this iron resides within the diffuse aggregate structure and so the volume fraction ϕ_{Hg} of mercury, bound or trapped within the aggregate is given by $\phi_{agg} - \phi_{Fe}$. Hence $\phi_{Hg} \sim 0.48$.

Since however $\rho_{agg} = \rho_{Hg} \phi_{Hg} + \rho_{Fe} \phi_{Fe}$,

$\rho_{agg} \sim 13.32 \text{ grms cm}^{-3}$. This value of ρ_{agg} may be substituted in the equation (7.3), giving a $\sim 2 \times 10^{-4} \text{ cm}$. This demonstrates that the size of the aggregate determined from settling experiments is not particularly dependent upon the actual aggregate density. Moreover a $\sim 10^{-4} \text{ cm}$ is in agreement with aggregate sizes determined from time dependent magnetisation experiments for similar fluids.

8. THE RESISTIVITY OF IRON PARTICLES IN MERCURY LIQUIDS

The fluids described in this section have all been prepared in the usual manner by electrodeposition, and their electrical resistivity measured between 77K and 300K using a conventional four probe method with current reversal.

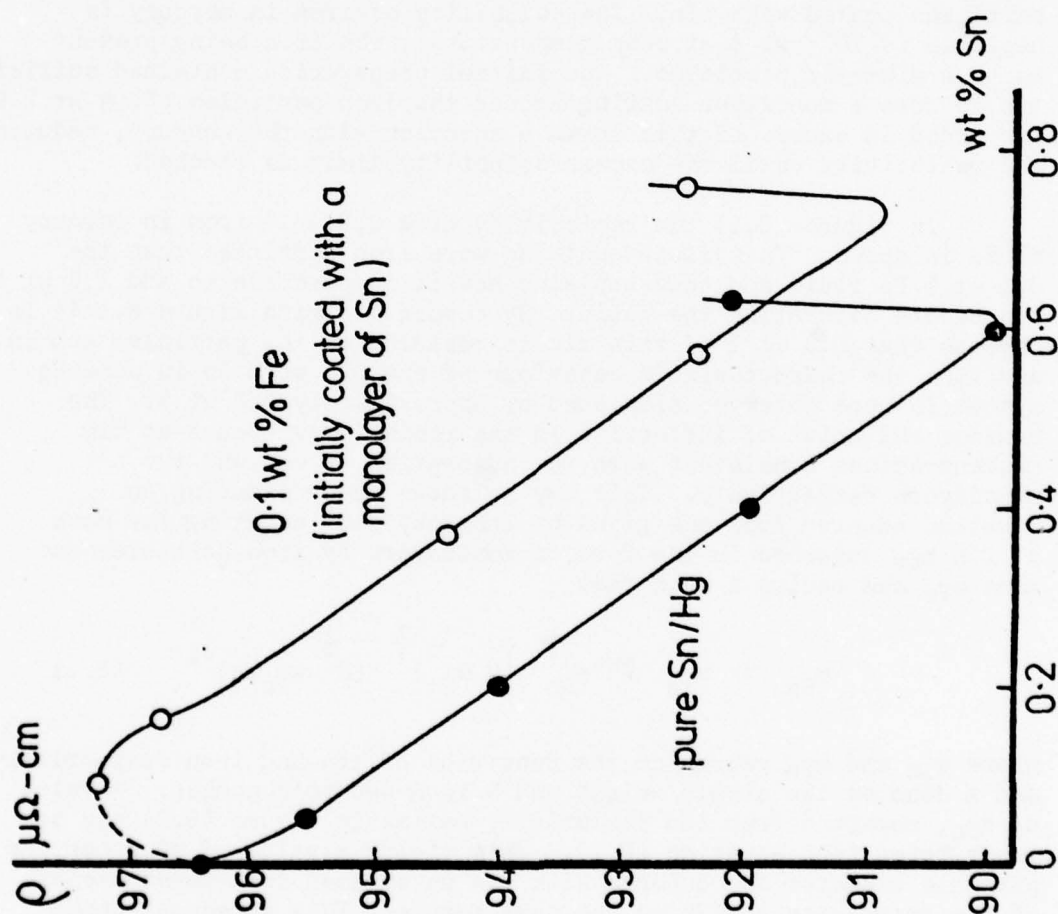
The lower curve of figure (8.1) shows the effect on the resistivity of adding free tin to pure mercury, at room temperature. A simple linear depression of the fluid resistivity with tin concentration is observed provided that the tin concentration remains less than 0.6 wt % (the saturation limit). Above this concentration there is a sharp increase in the resistivity. The upper curve of figure (8.1) shows a similar resistivity plot for a fluid containing 0.1 wt % iron particles coated with tin. The solubility of iron in mercury is negligible ($< 10^{-7}$ wt % at room temperature); the iron being present as 40 Å diameter particles. The initial preparation contained sufficient tin to form a monolayer coating around the iron particles (0.04 wt % Sn). Tin added in excess of this forms a solution with the mercury, reducing the resistivity until the excess solubility limit is reached.

In figure (8.2) the resistivity of a 0.8 wt % iron in mercury fluid is shown. This fluid contains more iron particles than the 0.1 wt % Fe fluid and thus explains how it is possible to add 1.2 wt % tin before saturating the fluid. By comparison with figure 8.1 it is obvious that 0.6 wt % of this tin is residing on the particles and in addition the characteristic behaviour of the 0.6 wt % Sn in pure Hg system is here observed displaced by approximately 0.6 wt %. The maximum and point of inflection in the resistivity occurs at tin concentrations consistent with the adsorption of one and two monolayers respectively. This may be shown by considering an equation adapted from one given by Luborsky (15) equating the mass of tin m_{Sn} adsorbed in the form of monolayers by iron particles and mass m_{Fe} and radius a such that

$$m_{Sn} = m_{Fe} \sqrt{3} A_{Sn}^{\frac{1}{3}} (2 w_{Sn})^{\frac{2}{3}} (N^{\frac{1}{3}} w_{Fe} a)^{-1} \quad (8.1)$$

where w_{Sn} and w_{Fe} represent the densities of tin and iron respectively and A denotes the atomic weight and N is Avogadro's number. A value of m_{Sn} , obtained from the resistivity maxima in figure (8.2) may be substituted into equation (8.1). This yields a value of 40 Å for the particle diameter as compared with 35 Å determined from measurements of the coercivity at 77K on the same sample. This agreement lends support to assumptions that the resistivity maxima corresponds to the adsorption of a monolayer of tin. Further, this association may be explained by using the theory of Lang (16) which relates charge transfer and changes in substrate work functions to metallic adsorbate coverage.

Figure (8.1) shows the depression in the resistivity of pure mercury and of a fluid initially coated with a monolayer of tin, when excess tin has been added.



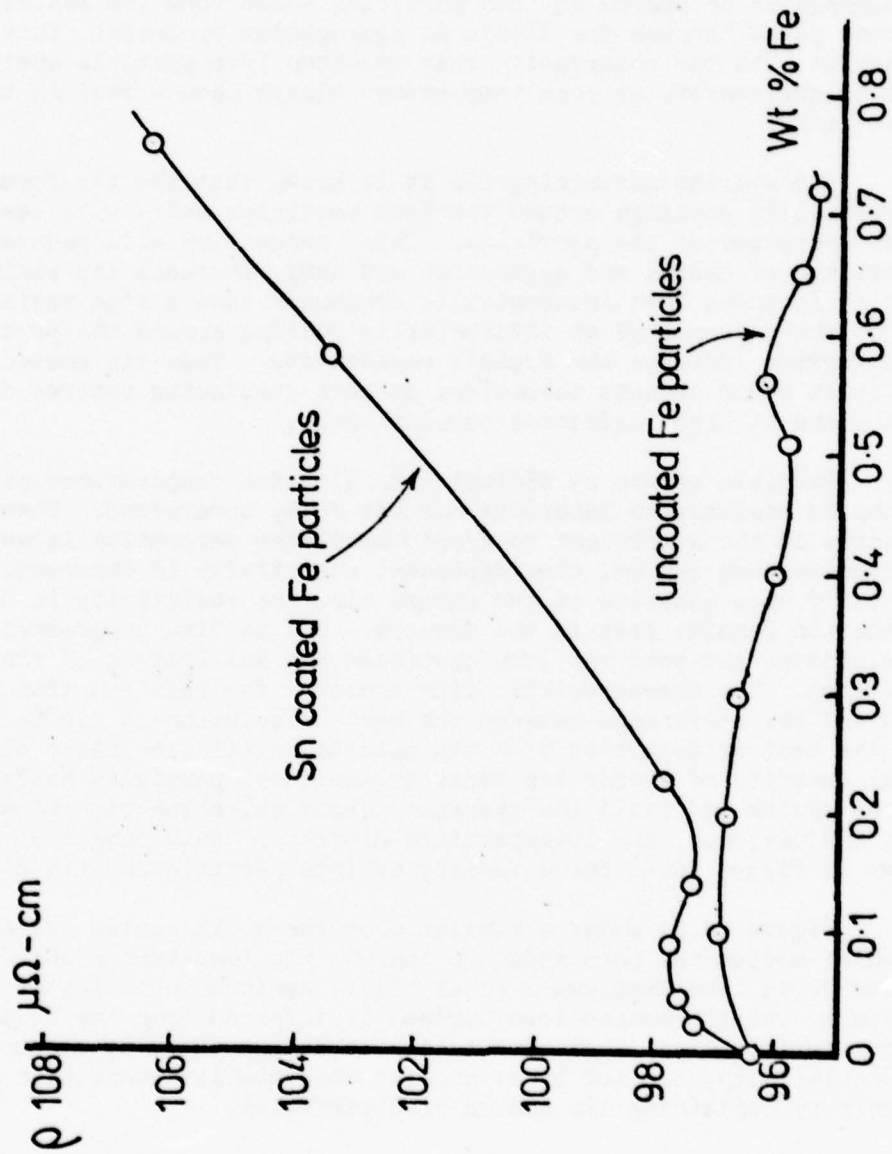


Figure (8.3) shows the variation of the resistivity for uncoated and tin-coated iron particles as the iron particle concentration is increased.

Popplewell et al (1), Hoon et al (6). Because of the larger difference in the work functions at a tin coated iron/mercury interface to that of an iron/mercury one, more charge transfer (and thus more conduction electron scattering) may be expected. This was the explanation proposed by Hoon et al (6) in relation to the resistivity behaviour seen in figure (8.3). It is now proposed that the state of aggregation may also be important. As the resistivity of iron is less than that of mercury by a factor of ten, the formation of aggregates or chains of iron particles would form low resistance current paths through the liquid as aggregation proceeds. This is in agreement with the observation that uncoated iron particle systems left to agglomerate at room temperature always show a fall in the resistivity.

For systems containing tin it is known that the tin forms intermetallic coatings around the iron particles which will lead to a separation of the particles. This separation will reduce the importance of chains and aggregates and hence increase the resistivity. Also it is known that intermetallic compounds have a high resistivity and so the presence of an intermetallic coating around the particle will further increase the fluid's resistivity. Thus tin coated particles would present themselves as both scattering centres due to charge layers and as high resistance current paths.

Particle growth by diffusion at elevated temperatures produces a complex resistivity behaviour not yet fully understood. When a quantity of tin sufficient to exceed monolayer saturation is added to an iron-mercury system, time dependent resistivity is observed. Initially upon addition of the excess tin, the resistivity is depressed as the tin remains free in the mercury. But as time progresses the tin precipitates out onto the iron particles and multilayers of tin will form. The characteristic time constant for this reaction depends upon (i) the difference between the heat of solution of tin in mercury and the heat of formation of a tin multilayer (ii) the ratio of the total quantity of excess tin added to the total particles surface area of the system and (iii) the distance across which the tin atoms must diffuse; i.e. the interparticle distance. Such behaviour is shown in figure (8.4) for a variety of iron particle and tin concentrations.

Figure (8.5) shows a similar plot for a tin coated system to which sodium has been added to improve the long-term stability of the fluid (see Popplewell et al (1)). Again association of the sodium to the tin coated iron surface is inferred from the behaviour of the resistivity. Small quantities of sodium added to mercury increase its resistivity, but not by as much as when similar quantities are added to mercury containing tin coated iron particles.

It is pertinent to discuss here some magnetic concentration experiments. Iron particle fluids to which sufficient tin has been added to form a monolayer have been magnetically concentrated. The residual non-magnetic phase has been shown to consist entirely of mercury, by measurements of its resistivity and chemical analysis. The same experiment

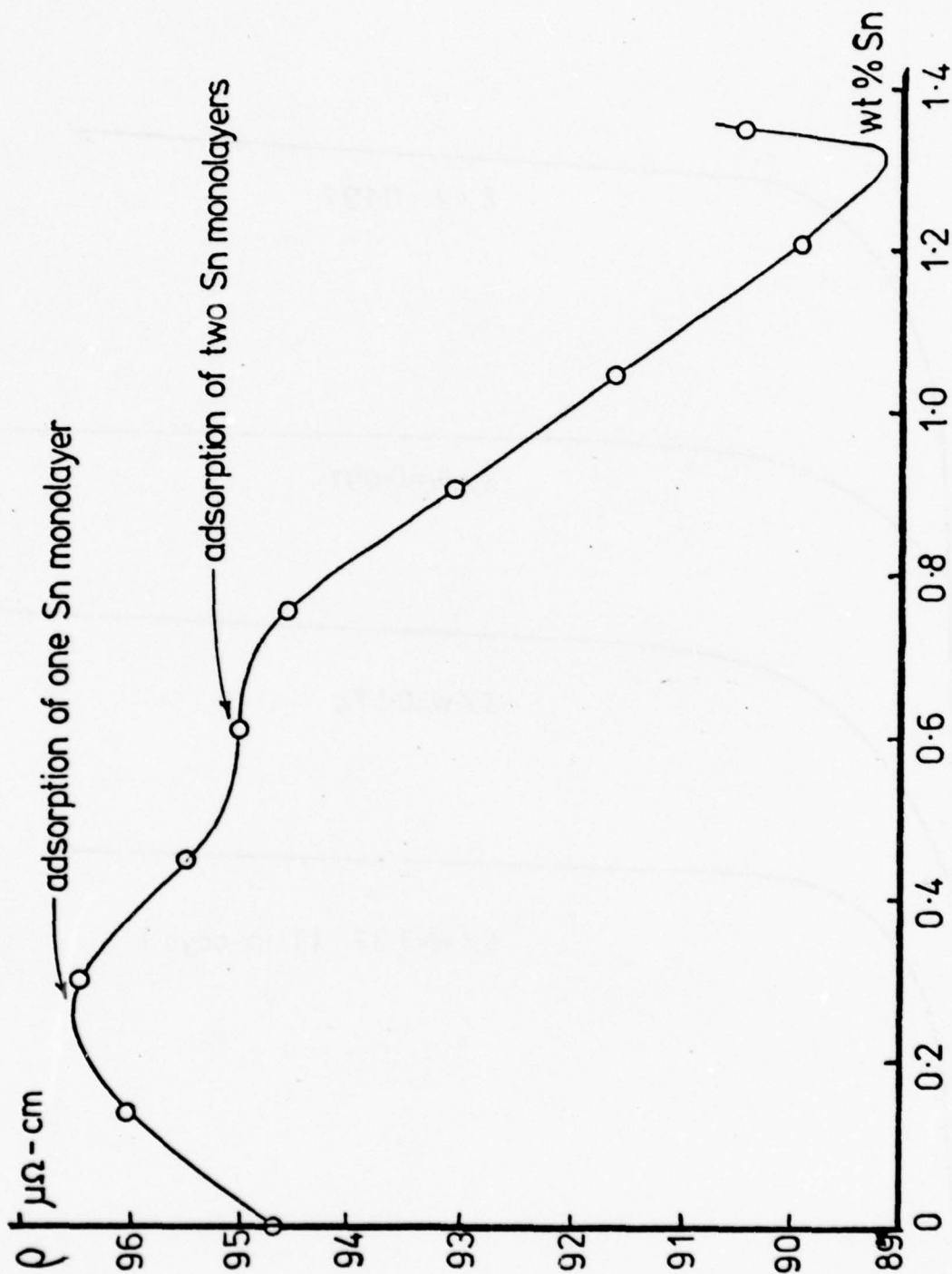


Figure (8.2) shows the variation in resistivity of an initially uncoated iron particle in mercury fluid, as tin has been added.

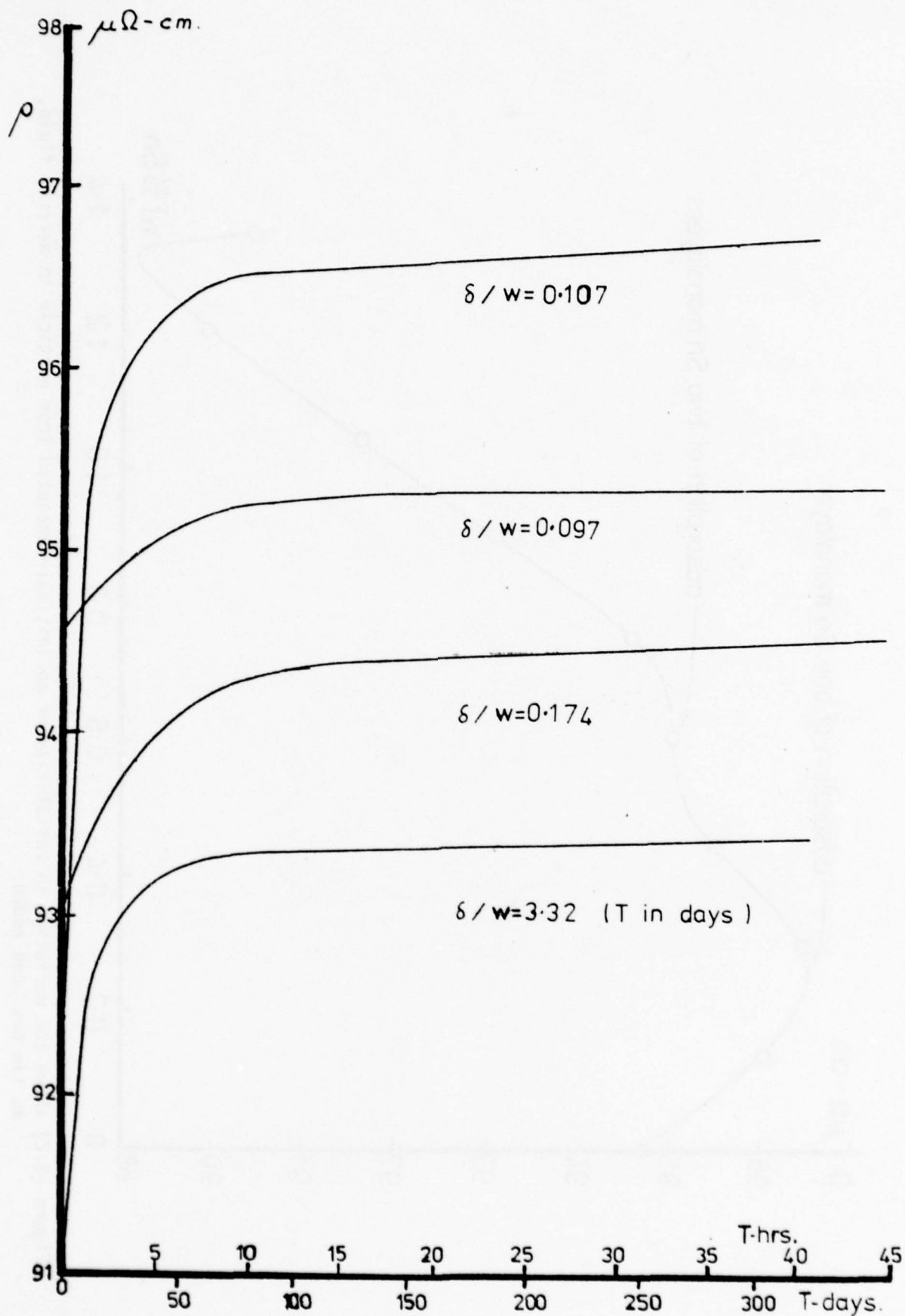


Figure (8.4) shows the time dependent resistivity observed for tin-coated iron particles, of weight % w ; where excess tin, of weight % δ , has been added to the fluids at $t = 0$.

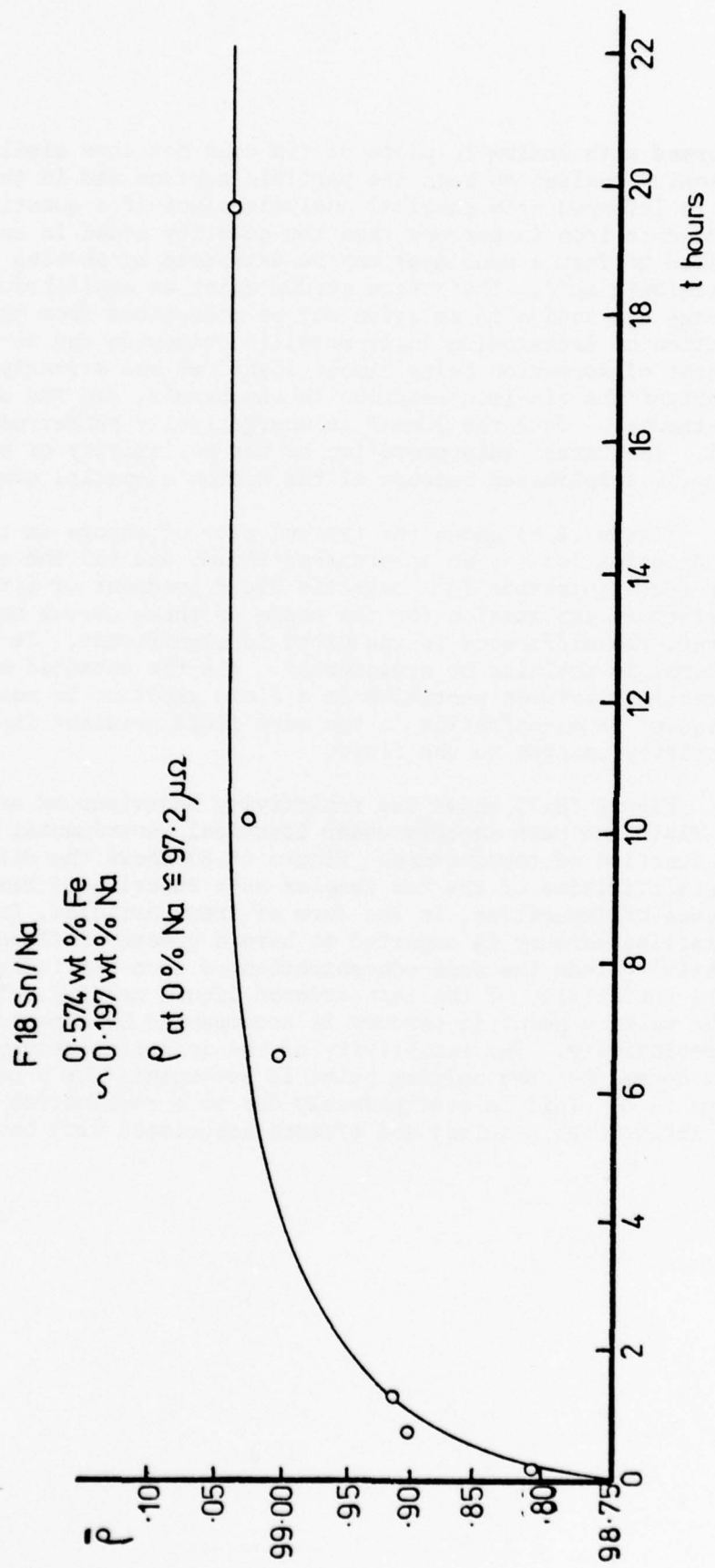


Figure (8.5) shows the time dependent variation in the resistivity of a tin coated iron particle fluid to which sodium has been added at $t = 0$.

performed with sodium in place of tin does not show similar results. The sodium resides on both the particle surface and in the mercury. This is inferred from chemical analysis since if a quantity of sodium is added to iron in mercury then the quantity added in excess of that required to form a monolayer may be extracted by shaking with dilute hydrochloric acid. That there should exist an equilibrium between iron coverage and sodium in solution may be understood from the heats of formation of iron-sodium inter-metallic compounds and mercury-sodium alloys; the heat of formation being almost identical and strongly exothermic. In comparison the tin-iron reaction is exothermic, and the mercury-tin endo-thermic. Thus the former is energetically preferred (see Smithells (17)). The direct interpretation of the resistivity of systems containing sodium is complicated because of the sodium's spacial distribution.

Figure (8.6) shows the typical plot of change in the resistivity upon dilution for (a) an as-prepared fluid, and (b) the same fluid after reconcentration in a magnetic field gradient of 1.5 kG. No satisfactory explanation for the shape of these curves has been proposed. However, the difference in the plots is significant. It is likely that irreversible chaining or agglomeration via the enhanced magneto-static interactions between particles in a field gradient is responsible. Subsequent reconcentration in the same field gradient imparts no further resistivity changes to the fluid.

Figure (8.7) shows the resistivity behaviour of a tin coated iron fluid and pure mercury under identical experimental conditions as a function of temperature. Figure (8.8) shows the difference in the resistivities of the two samples as a function of temperature. The presence of impurities, in the form of iron particles, in the solid crystalline mercury is expected to have a greater influence upon the resistivity than the same concentration of iron particles would have on the resistivity of the less ordered liquid mercury. The approach to the melting point in mercury is accompanied by a rapid change in the resistivity. The resistivity of the iron-tin-mercury system as it approaches the melting point is accompanied by a more gradual change in ρ . This is most probably due to a combination of pre-melting (see latent heat results) and effects associated with bound mercury.

Resistivity of 30A diameter particles of Iron in Mercury

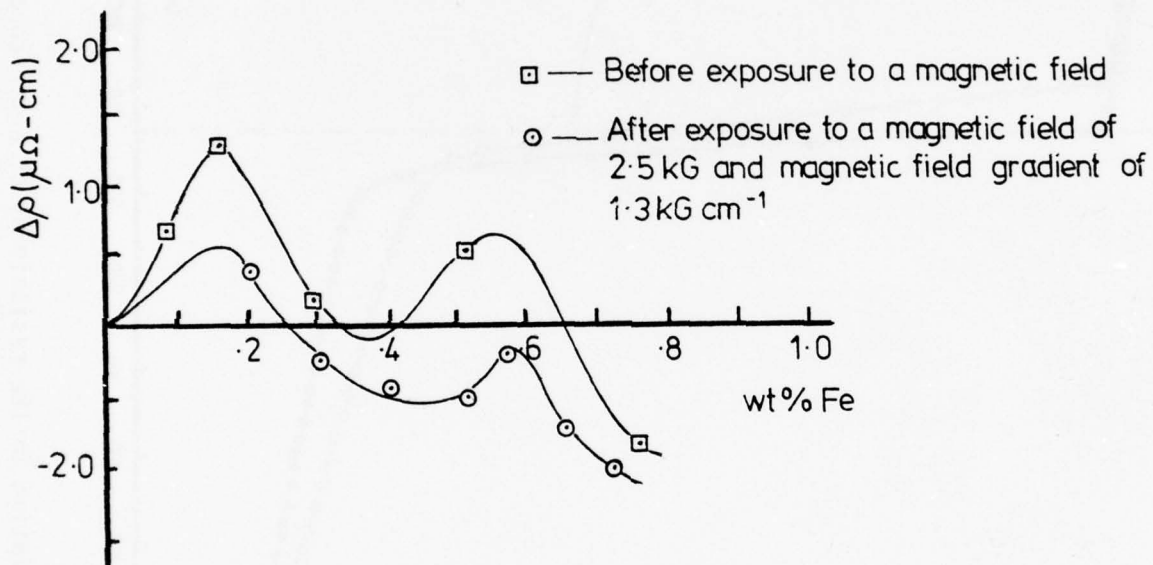


Figure (8.6) shows the variation in the resistivity for an iron particle in mercury fluid as the concentration is decreased (i) before exposure to a magnetic field and (ii) after reconcentration in a magnetic field gradient.

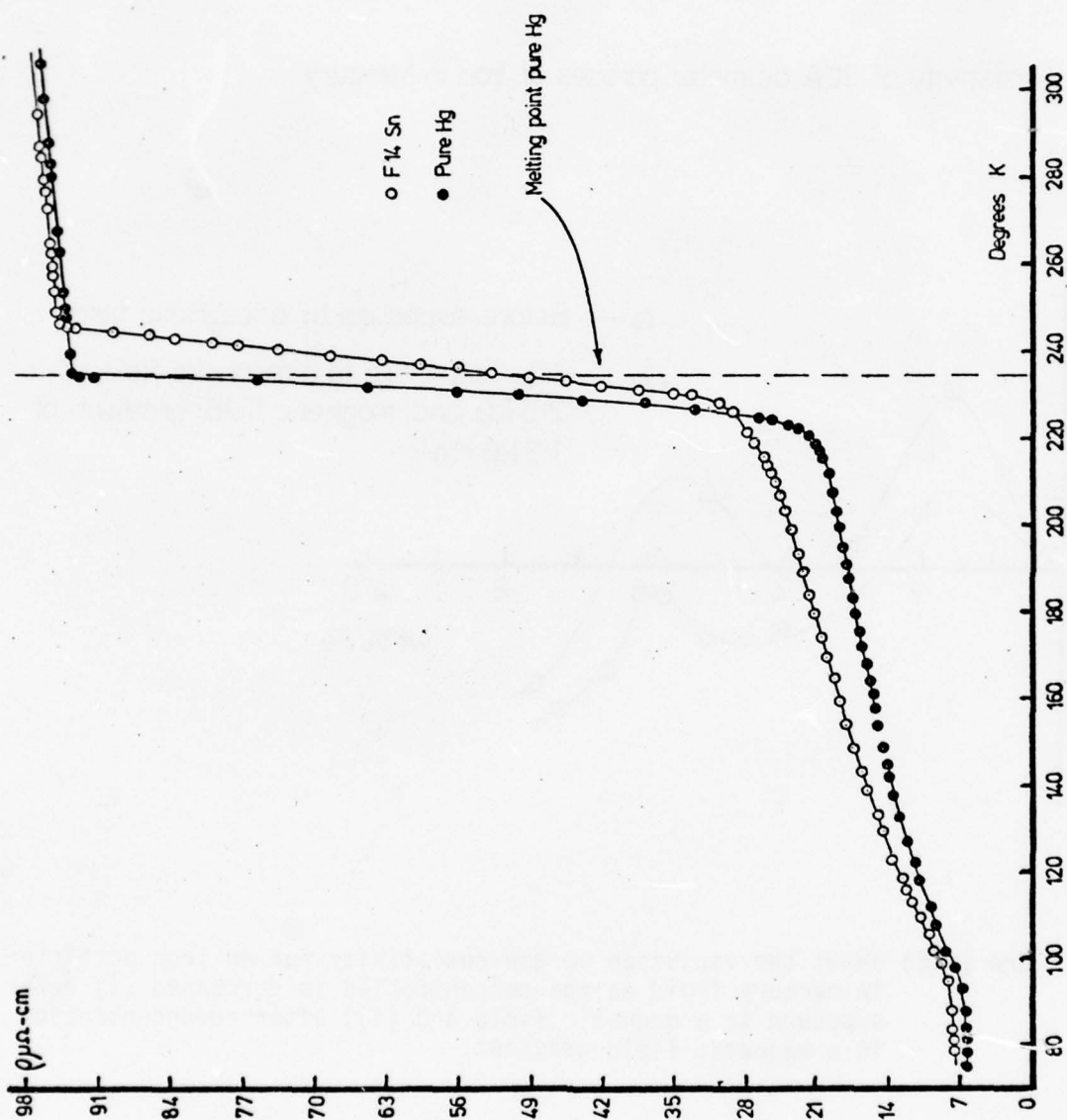


Figure (8.7) shows the variation in the resistivity of a tin-coated iron particle fluid in mercury and pure mercury as a function of temperature.

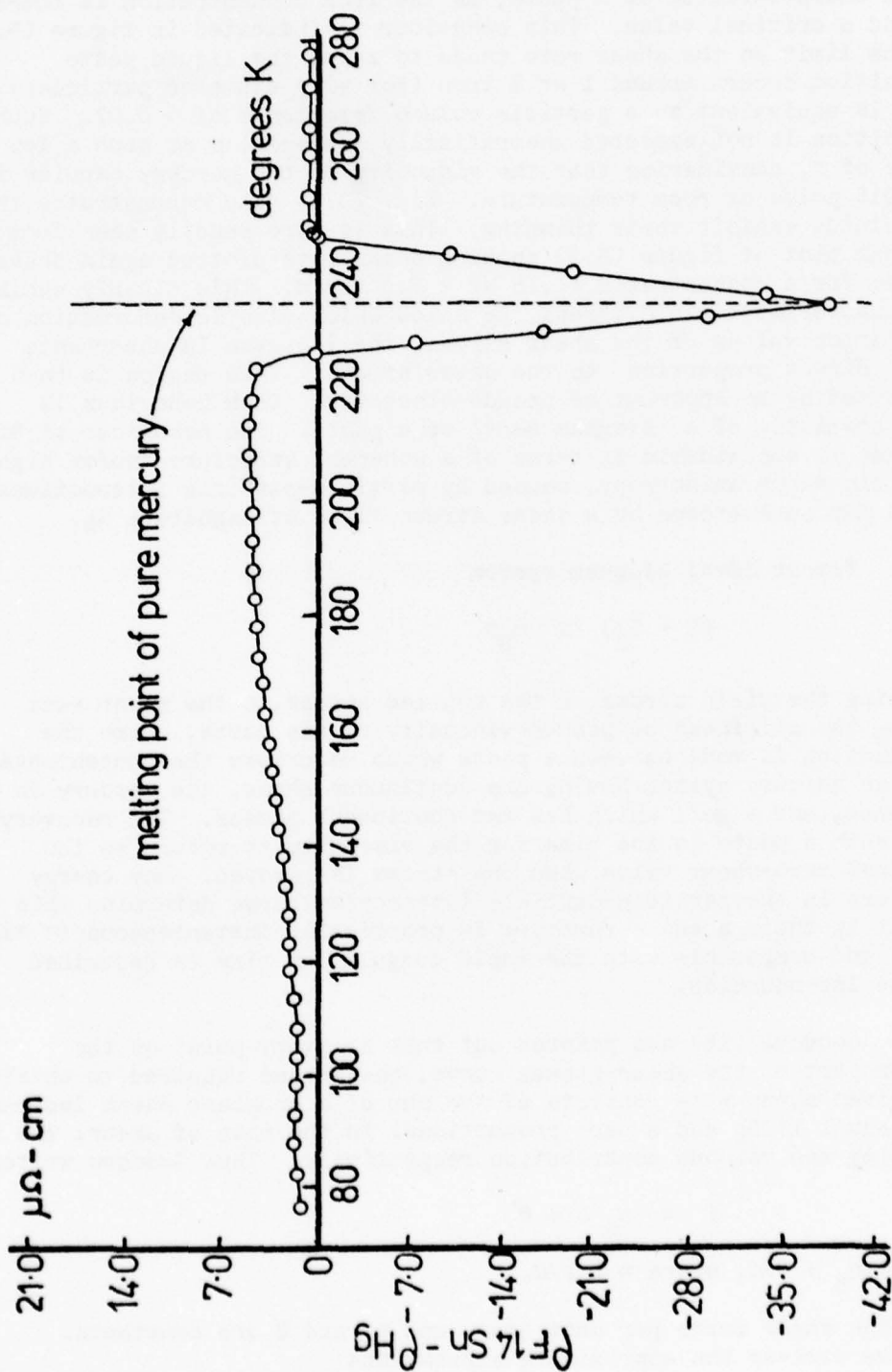


Figure (8.8) shows the difference in the resistivities of a tin-coated iron particle in mercury fluid and pure mercury at the same temperature.

9. VISCOSITY MEASUREMENTS

The most striking feature of the viscosity of a ferromagnetic liquid containing iron particles in mercury is the transition from a low value of the viscosity η characteristic of a liquid to a high value characteristic of a paste, as the iron concentration is increased beyond a critical value. This behaviour is indicated in figure (9.1). In the limit as the shear rate tends to zero, the liquid-paste transition occurs around 1 wt % iron (for 40 Å diameter particles). This is equivalent to a particle volume fraction ϵ of ~ 0.02 . Such a transition is not expected theoretically, especially at such a low value of ϵ , considering that the viscosity of the mercury carrier is ~ 0.015 poise at room temperature. Fig. (9.2) also demonstrates that the fluids exhibit shear thinning. This is more readily seen from the Bingham plot of figure (9.3) showing shear rate plotted against shear stress for a concentrated (1.15 wt % Fe) fluid. This clearly exhibits a characteristic yield stress, S_B below which elastic deformation occurs. For larger values of the shear stress, the increase in shear rate is in direct proportion to the shear stress. This region is then described by an apparent or pseudo-viscosity. Such behaviour is characteristic of a 'Bingham Body' or a paste. The behaviour of Bingham systems is explainable in terms of a coherent structure and/or high particle shape anisotropy, caused by particle-particle interactions which may be overcome by a shear stress field of magnitude S_B .

For an ideal Bingham system

$$(S - S_B) = \eta_B \sigma$$

S_B being the yield stress, S the applied stress, σ the shear rate and η_B the stiffness or pseudo-viscosity of the paste. Here the distinction is made between a paste which describes the concentrated iron in mercury system having one continuous phase, the mercury in this instance, and a gel which has two continuous phases. The recovery time τ' of such a paste is the time for the viscosity to return to the original zero-shear value when the stress is removed. Any energy barriers in the particle-particle interaction curve determine this time τ' , but in their absence recovery is practically instantaneous ($\tau' \sim 10^{-6}$ secs) and comparable with the rapid coagulation time as described in the Introduction.

Goodeve (18) has pointed out that at every point on the linear part of the shear-stress curve, the stress required to obtain the given shear rate consists of the sum of a constant shear independent part equal to S_B and a part proportional to the rate of shear; the bond breaking and viscous contribution respectively. Thus Goodeve writes,

$$F = \eta_s \sigma + \theta'$$

or $\eta = \eta_s + \theta'/\sigma$, where $\eta \equiv F/\sigma$.

F is the shear force per unit area, and η_s and θ' are constants. Goodeve derives the approximate expressions

Viscosity vs wt % Fe 45 Å particles uncoated
(at given shear rates in cm/sec/cm)

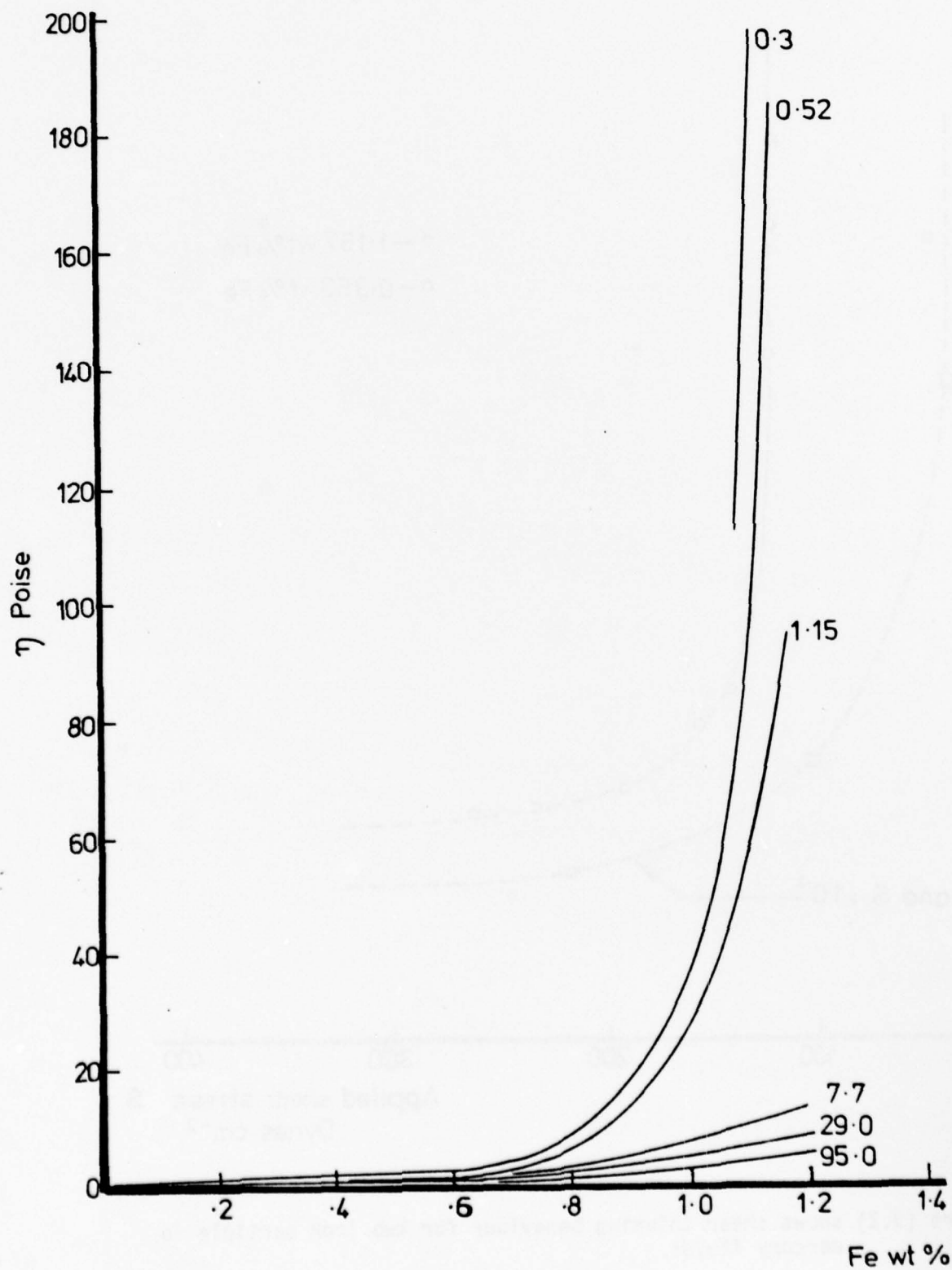


Figure (9.1) shows the variation in the viscosity of an iron particle fluid as a function of iron concentration, at specified shear rates, (sec⁻¹).

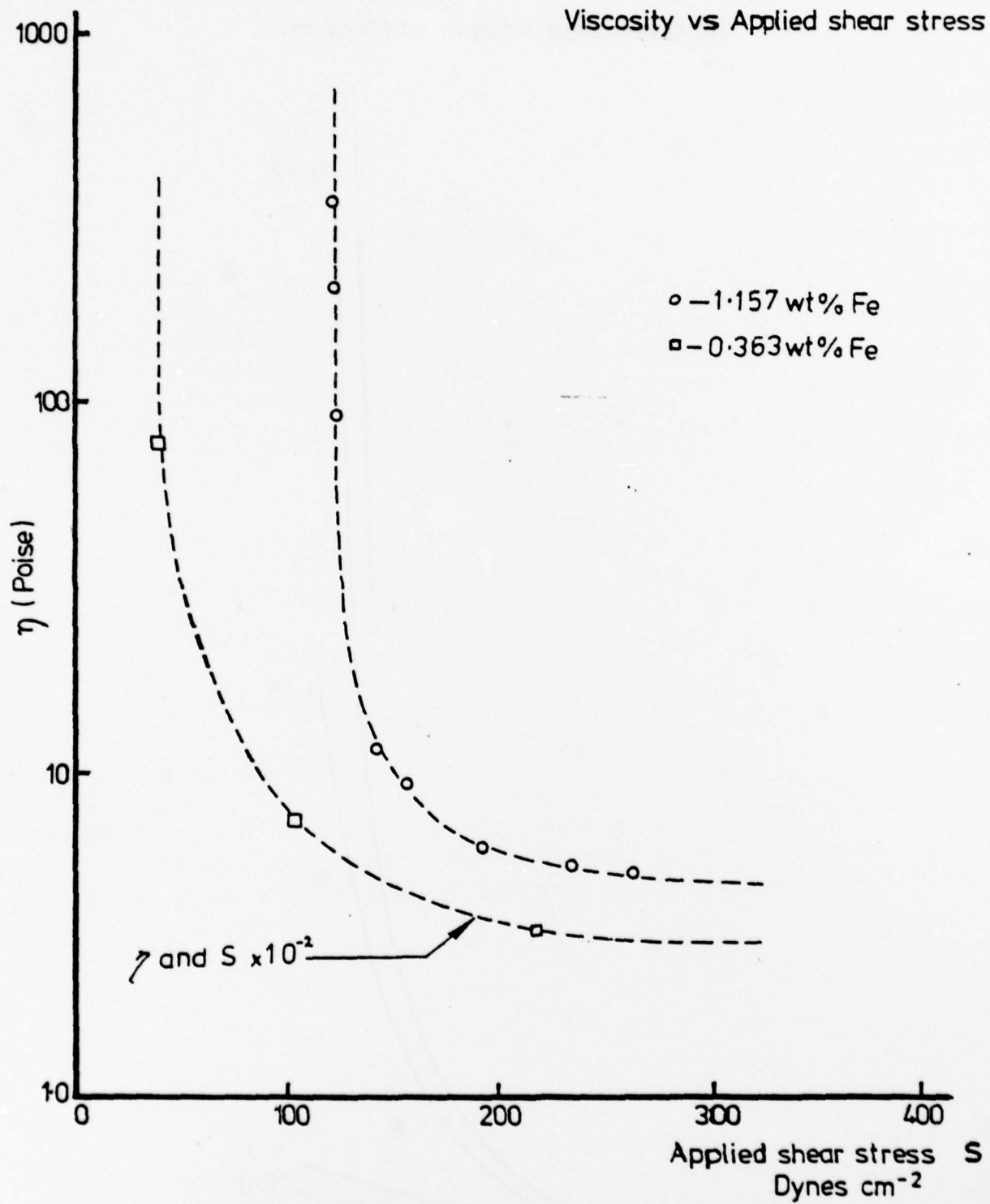


Figure (9.2) shows shear thinning behaviour for two iron particle in mercury fluids.

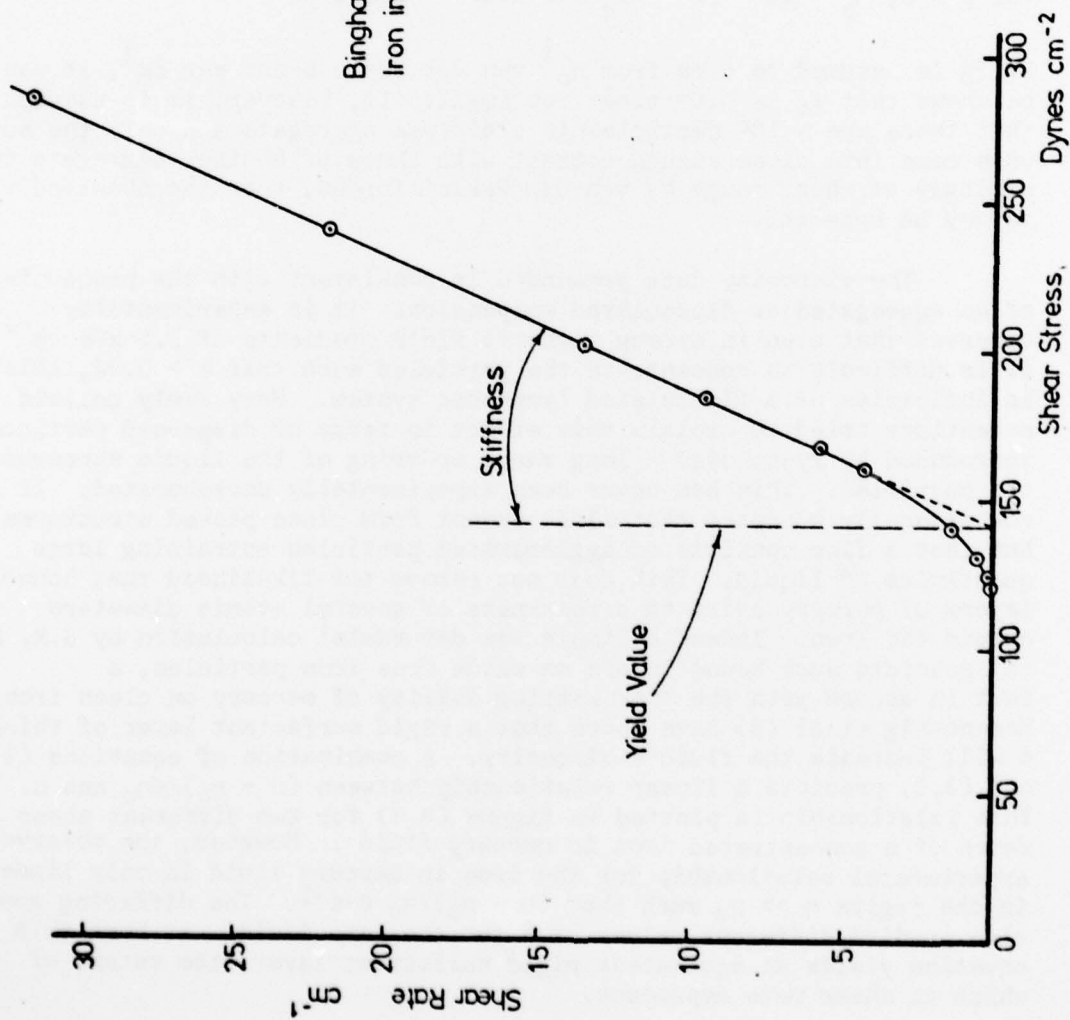


Figure (9.3) shows the 'Bingham fluid' behaviour for a 1.157 wt% iron particle in mercury fluid.

$$\theta' = \frac{1}{2} f_c n' Z$$

and $S_B = f_c n' Z$

where n' is the number of links or bonds per cm^{-3} , Z is a length characteristic of the particle separation, which Goodeve states may decrease with increasing shear rate, f_c is the maximum force a link can withstand in the direction of shear. Thus S_B can be used to compute f_c for a given particle concentration. If it is assumed that the iron particles are individual and isotropically dispersed then $Z \sim n_0^{-1/3}$, where n_0 is the number of particles per cm^3 , and $n' \sim \frac{1}{2} p n_0$ where p is the particle co-ordination number. Thus

$$f_c \sim 2S_B / p n_0^{2/3}$$

For $p = 6$, $n_0 \sim 10^{17} \text{ cm}^{-3}$ $f_c \sim 2 \times 10^{-10} \text{ dynes/cm}^2$.

If f_c is assumed to come from $n_0^{2/3}$ van der Waals bonds per cm^2 , it can be shown that f_c is $\sim 10^4$ times too small. If, however, it is assumed that there are $\sim 10^6$ particles in a diffuse aggregate and only the outer ones come into close enough contact with those of another aggregate to bond strongly at short range by van der Waals' forces, then the observed value of f_c may be expected.

The viscosity data presented is consistent with the properties of an aggregated or flocculated suspension. It is experimentally observed that even in strong magnetic field gradients of 1.5 kOe cm^{-1} it is difficult to concentrate the particles such that $\epsilon > 0.02$, this is indicative of a flocculated lyophobic system. Many early colloid scientists tried to explain this effect in terms of dispersed particles surrounded by lyospheres - long range ordering of the liquid surrounding the particles. This has never been experimentally corroborated. It is now generally accepted that flocs cannot form close packed structures but that a floc consists of agglomerated particles entraining large quantities of liquid. This does not remove the likelihood that bound layers of mercury exist to a thickness of several atomic diameters around the iron. Indeed a simple van der Waals' calculation by S.R. Hoon (5) predicts such bound layers on oxide free iron particles, a fact in accord with the known wetting ability of mercury on clean iron. Rosensweig et al (3) have shown that a rigid surfactant layer of thickness δ will increase the fluid's viscosity. A combination of equations (3.2) and (3.3) predicts a linear relationship between $(\eta - \eta_0)/\epsilon \eta_0$ and ϵ . This relationship is plotted in figure (9.4) for two different shear rates of a concentrated iron in mercury fluid. However, the observed experimental relationship for the iron in mercury fluid is only linear in the region $\eta \gg \eta_0$ such that $(\eta - \eta_0)/\eta_0 \epsilon \epsilon^{-1}$. The differing gradients also predict different values of δ for the same fluid. At best this equation yields an equivalent rigid surfactant layer, the extent of which is shear rate dependent.

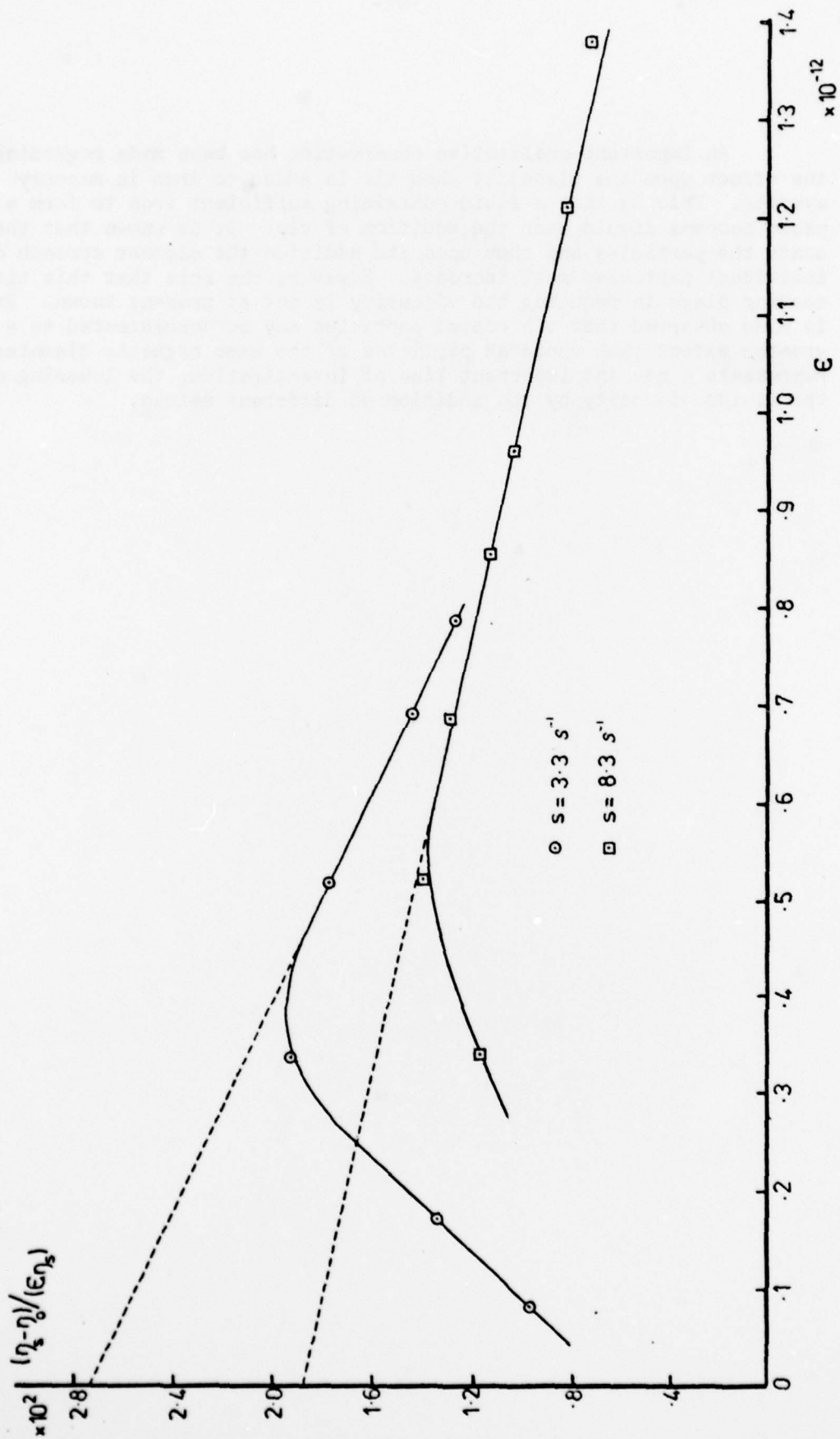


Figure (9.4) shows the very limited validity of the equations (3.2) and (3.3) in explaining the observed viscosity of iron particles in mercury.

An important qualitative observation has been made regarding the effect upon the viscosity when tin is added to iron in mercury systems. This is that a fluid containing sufficient iron to form a paste becomes liquid upon the addition of tin. It is known that the tin coats the particles and thus upon its addition the closest approach of individual particles must increase. However, the role that this tin coating plays in reducing the viscosity is not at present known. It is also observed that tin coated particles may be concentrated to a greater extent than uncoated particles of the same magnetic diameter. This represents a new and important line of investigation, the lowering of the fluids viscosity by the addition of different metals.

10. PHASE CHANGES AT THE MELTING POINT

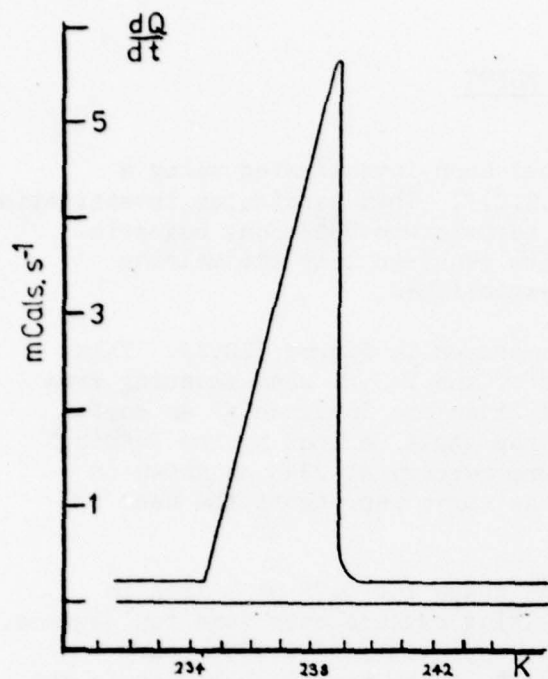
The solid-liquid transition has been investigated using a differential scanning calorimeter (D.S.C.). This particular investigation arose as a result of observations of temperature dependent magnetic measurements where the analysis of data required that the melting point of the iron-mercury system be established.

The principal results are summarised in figure (10.1). This figure shows the line shapes produced by the D.S.C. when scanning from low to high temperatures. Isothermal lines are inclined at an angle ψ to the line shape base line. ψ is the angle defined by the leading edge for the melting transition of pure mercury at 234K as shown in figure (10.1.1). The total area of the curve represents the heat of fusion.

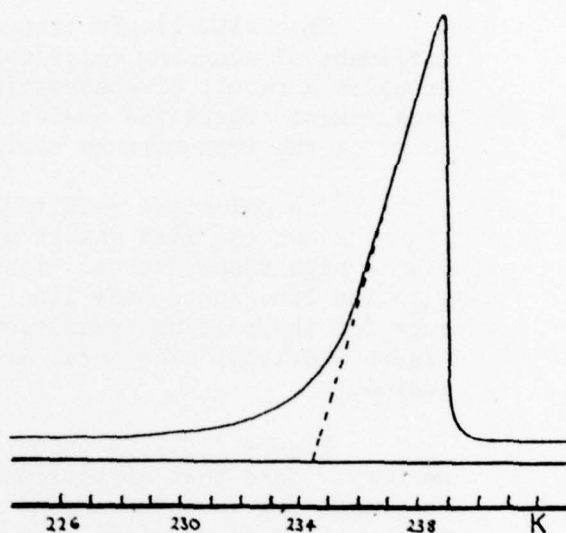
Figure (10.1.2) shows the line shape for 0.75 wt % iron in mercury. Note that significant premelting extends over some ten degrees. No premelting is observed, as would be expected for 99.999% pure mercury (see figure (10.1.1)). The area of the premelted region ie the area to the left of the dotted line in figures (10.1.2) and (10.1.3) is normally a measure of the impurity of the system and is designated by Q_p .

Figure (10.1.3) shows the results for a fluid containing tin coated iron particles with an identical particle concentration to the fluid studied in figure (10.1.2). The premelting curve shows a bump which is characteristic of all tin coated iron fluids, but it is of unknown cause. In marked contrast is the line shape for figure (10.1.4) for free tin in mercury of the same concentration as that present in figure (10.1.3). Here structure appears to the right of the melting point and represents the heat of transition from β tin in mercury to tin in solution in liquid mercury. This structure always exists when free tin is present but never if iron particles are also present. This would seem to indicate that tin is not in solution in the fluids containing iron particles but is associated with the particles as a coating. This result is consistent with the results of the measurements of resistivity of the fluids described in section (9).

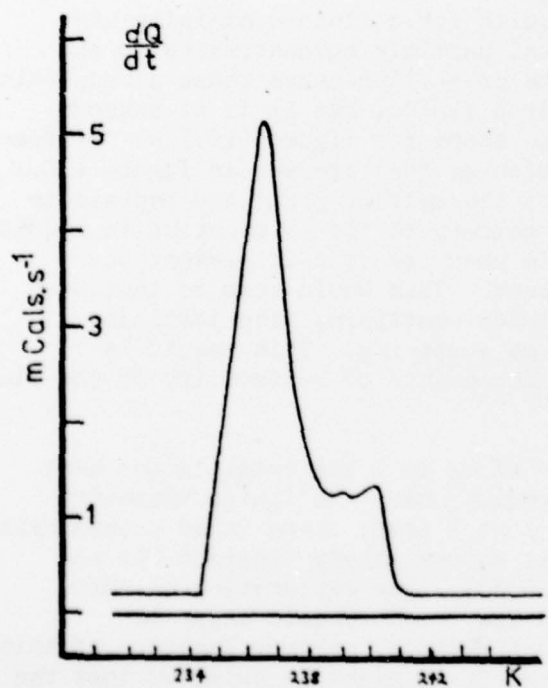
Figure (10.2) shows the ratio of Q_p to Q the total latent heat of transition. It is seen that the region where the fluids viscosity becomes paste-like, at approximately 1 wt % iron, there is an accompanying sharp increase in Q_p , even though Q is approximately constant for all concentrations of iron (see figure (10.3)). One explanation of this is that the amount of free mercury in the thermodynamic sense is decreasing as it is gradually used to form bound mercury layers. If this were the sole cause of the behaviour of Q_p it might be expected that the total latent heat Q of the sample would also change with change of iron concentration. Figure (10.3) shows that this is not the case. However,



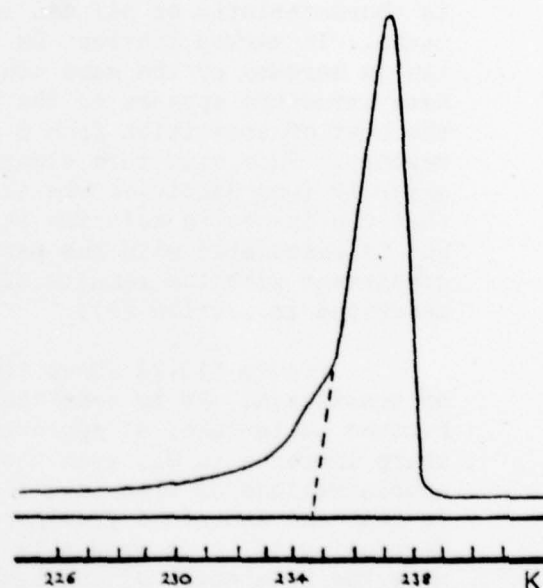
(1.) PURE Hg



(2.) Fe PARTICLES (0.75wt%) IN Hg



(3.) 0.4wt% Sn IN Hg



(4.) Sn COATED Fe PARTICLES IN Hg
(0.4wt% Sn , 0.75wt% Fe)

Figure (10.1) shows the line shapes for various samples produced by the D.S.C. as the samples are melted.

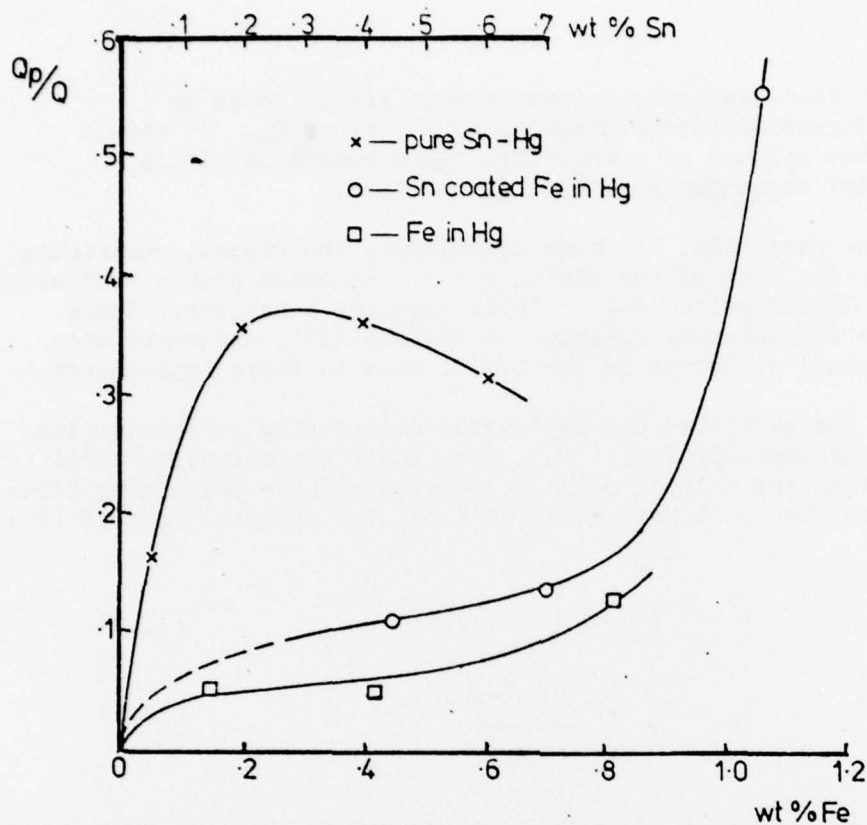


Figure (10.2)

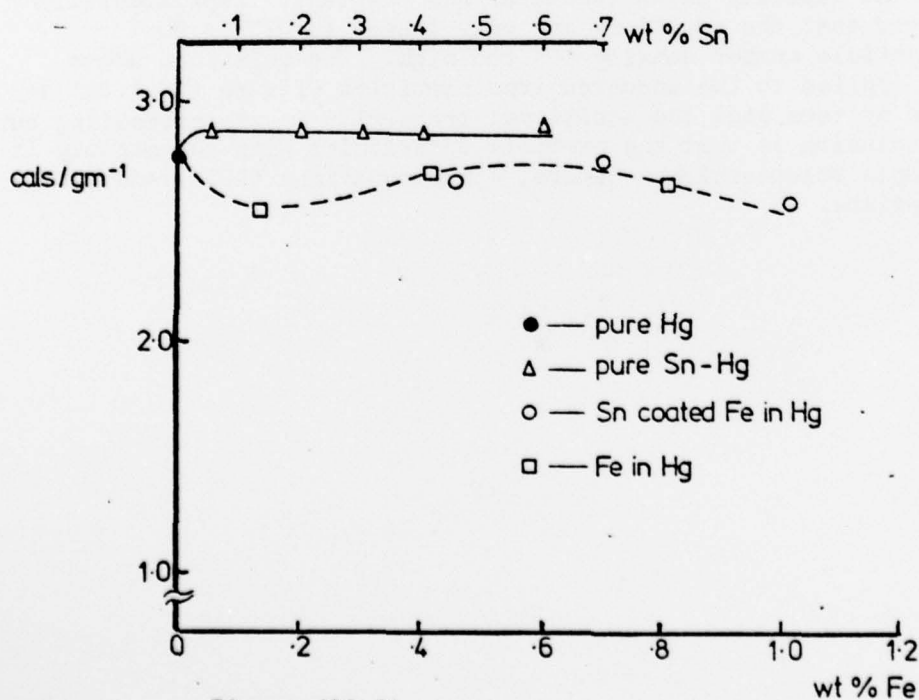


Figure (10.3)

Figure (10.2) shows the ratio of premelting heat to total heat of transition as a function of iron and tin concentration.

Figure (10.3) shows the total heats of transitions as a function of iron and tin concentration.

the role of particle interactions is most likely to be an important factor in determining the behaviour of Q_p . It should be noted that because of premelting, there exists no single melting point characteristic of a given fluid.

Fine particles, if thermodynamically individual, contribute to the specific heat of the fluid, due to increased phonon scattering and in the liquid state, due to their gas-like behaviour. These effects are discussed by Novotny and Meincke (19), and may be seen to be too small to detect on the D.S.C. used in these experiments.

If the particles can be treated as impurity macromolecules, each thermodynamically individual, then their concentration should determine both the melting point depression and the premelting behaviour according to the van't Hoff equation (see, for example, Rossini (20)) such that

$$T = T_o - (T_o - T_m) F^{-1} \quad (10.1)$$

$$\text{and} \quad T_o - T_m = \frac{R T_o^2 x}{H} \quad (10.2)$$

Where F is the fraction of sample melted at T , $T_o - T_m$ the depressed melting point, H the pure substance molar heat of fusion, x the mole fraction of the impurity and R the molar gas constant. Experimentally it is observed that the equations are only linear for $F^{-1} < 20$ predict a particle number density 10^2 too high. The relations above may only be applied to the uncoated iron particles (figure (10.1.3)) as the iron-tin systems show the additional transition in the premelting curve. Thus the conclusion is that the particle interaction with the mercury is not of a simple solute-solvent nature, since equations (10.1) and (10.2) are inappropriate.

11. CONCLUDING REMARKS

The resistivity data, presented in section 8, has enabled the spatial location of the metallic additives; tin and sodium, to be determined. The data has shown differences in the behaviour of uncoated iron and tin-coated iron systems which have been attributed to either the existence of charge layers or high resistance intermetallic coatings or both. There is also evidence that the state of agglomeration modifies the resistivity behaviour of these fluids.

The presence of tin coatings has also been strikingly corroborated by latent heat measurements. From these measurements there also appears evidence for the existence of mercury bound layers, although not of large spatial extent. The existence of such layers would not be inconsistent with the reported temperature dependence of resistivity of iron particles in mercury.

It has been possible to study systematically some of the conditions that determine I_s , I_R , H_C and χ for a given sample, where I_s is the sample's saturation magnetisation, I_R the remanance, H_C the coercivity and χ_i the initial susceptibility. Each of these parameters is strongly affected by particle size distributions and interactions, crystal, shape and structural anisotropies.

It is possible that the magnetic and hydrodynamic particle sizes may differ widely. This could occur if aggregation of the particles occurred. The presence of aggregates in the fluids has been confirmed and their size determined from measurements of the fluid stability in a gravitational field (see section (7)). The dilution and demagnetising field experiments of section (5) imply that the magnetic behaviour of the aggregates is affected appreciably by nearest neighbour interactions. The time dependent magnetic data of section (6) can only be understood in terms of the existence of large aggregates. This implies strong nearest neighbour interactions, since for the fluids at room temperature, it is easier to rotate the aggregate than the individual particle moments.

It should be noted that the viscosity data presented in section (9) cannot be explained by theories which assume that the iron particles are hydrodynamically separate or loosely interacting entities. The viscosity behaviour may, however, be explained in terms of aggregates, especially open structured aggregates (ie. flocs). It is then unnecessary to talk of bound mercury layers of the order of 50 Å on the iron particles' surface in order to explain the paste-like nature of fluids which contain 1 wt %, 40 Å diameter iron particles in mercury. Open aggregates would also explain the magnetic field gradient instability, where the observed particle transport rate is orders of magnitude faster than that predicted from the iron particle diameters obtained from coercivity measurements.

It has also been observed that the addition of tin reduces the viscosity of the fluid, a fact which must be related to the coating ability of the tin. The lowering of the viscosity by the addition of

further materials (such as antimony) which are also known to coat the iron particles would represent a new area of experimental investigation.

In summary it may be said that the magnetic resistivity, latent heat, viscosity and gravitational stability experiments have enabled the iron particle interactions in mercury to be investigated. It is now apparent that the existence of aggregates determines many of the properties of the fluids. The forces determining the formation of the aggregates may be considered to be (i) short range van der Waals forces and (ii) longer range magnetic forces. As a result of these studies a more realistic model of the iron-mercury fluids has evolved; a development fundamental to the progress of further work.

12. FUTURE WORK

Evidence has been presented that the high viscosity of iron in mercury fluids is related to the tendency of the particles to aggregate. Ultimately the stability of the iron-mercury systems depends on the magnitude and spatial dependence of both magnetic and van der Waal's forces, the latter being primarily responsible for particle agglomeration in these systems. It is necessary, therefore, to reduce the van der Waal's force or counteract it with a repulsive force if stability is to be achieved. A repulsive force between particles could be provided by producing a charged surface layer on the particle, analagous to the charged double layer in colloids. This has been discussed in section (3). However, it is necessary that the difference in work functions of the particle and carrier should be large if the repulsion is to be large. Hence the stability should be improved by adding sodium, which has a very different work function from iron or mercury, to the iron-mercury system. It appears, however, on the basis of experiment, that the repulsive forces are unable to prevent particle aggregation. Thus the effect of surface charge layers, in improving stability thought an attractive possibility still requires further study. Work is still continuing on this problem.

Certain metal additives effect the viscosity of iron-mercury systems. Tin, bismuth, magnesium and aluminium are reported to reduce the viscosity (21). Other metals are known to increase the viscosity. Metal additives which appear to reduce the viscosity may do so by reducing the van der Waals' forces between aggregates which is a necessary requirement for stability. A study of the effect of metal additives on both viscosity and stability will, therefore, form a substantial part of the next year's research programme.

As pointed out in section (3), some metal additives form coatings on the iron particles and reduce particle growth by diffusion. Tin is successful in this respect. Antimony is also expected to form particle coatings and reduce diffusional growth (Luborsky (15)) but in addition it is successful over a more extensive temperature range (up to 800 K). Hence it is important in the development of high temperature fluids to study the role of antimony metal as a stabilising additive in some detail. It is clear that metal additives have important effects on the physical properties and stability of iron-mercury systems. A systematic study of additives has formed a significant part of past research effort and work in this field must continue. Indeed, the most rewarding approach towards producing a stable metallic ferromagnetic liquid will be to identify a third element or compound which will both inhibit particle growth and prevent particle aggregation.

Finally, a parallel programme is being undertaken on ferromagnetic liquids with liquid gallium as the carrier, this being a suitable low melting point metal with possible high temperature application.

REFERENCES

1. J. Popplewell, S.W. Charles, and S.R. Hoon,
2nd Conference on 'Advances in Magnetic Materials and their
Applications' I.E.E. p.13-16 (Sept 1976).
2. H. De Bruyn (i) Proc of Int. Congress on Rheology, Holland,
1948, Amsterdam 1949, p.1195.
(ii) Rec. Trav. Chim. 61 (1942) 863.
3. R.E. Rosensweig, J.W. Nestor and R.S. Timmins:
A.I.Ch.E.-I. Chem. E. Symposium Series No.5, p.5:104 (1965)
4. M. von Smolowski (i) Physik Z., 17, p.557-585,(1916)
(ii) Z.Physik Chem., 92, p.129, (1917).
5. S.R. Hoon, Thesis, U.C.N.W., Bangor, Wales, U.K.
6. S.R. Hoon, J. Popplewell, and S.W. Charles
I.E.E. Transactions on Magnetics Vol Mag 14 No 5, 981-983 (1978)
7. P.L. Windle, J. Popplewell and S.W. Charles, I.E.E. Transactions on
Magnetics, Vol.11, 1367-1369 (1975).
8. G.W. Greenwood, Acta Met., 4, p.243 (1956).
9. R.W. Chantrell, J. Popplewell, S.W. Charles, Physica, 86-88B,
p.1421 (1977).
10. E. Kondorski (i) C.R. Acad.Sci., U.R.S.S. 80 p.197 (1951).
(ii) Bull.Acad.Sci., U.R.S.S. (Phys), 16, p.398 (1952).
11. F.E. Luborsky, J.A.P. Suppl., 32, p.1715 (1961).
12. M.I. Shliomis, Sov. Phys., U.S.P., 17, 2, 153 (1974).
13. T.B. Jones and D.A. Kruger, Office of Naval Research Report,
AD/A-001 107 September, 1974.
14. E.A. Peterson, D.A. Kruger, M.P. Perry and T.B. Jones, A.I.P. Conf.Proc
No. 24 p.560-561 (1975).
15. F.E. Luborsky, J.App.Phys., 33, p.2385 (1962).
16. N.D. Lang, Phys.Rev., 4, No.12, 4234 (1971).
17. C.J. Smithells, Metals Reference Book, Butterworths (1949).
18. C.F. Goodeve, Trans. Farad. Soc., 35, p.342-358 (1939).
19. V. Novotny and P.P. Meinke, Phys. Rev., 138, 4186 (1973).
20. F.D. Rossini, "Chemical Thermodynamics" p.294, John Wiley and Sons,
N.Y. (1950).
21. M. Flindt, U.S. Patent 3 130 004/1964.

Publications arising from the work sponsored by the U.S. Army

1. 'The Long Term Stability of Mercury Based Ferromagnetic Liquids', P.L. Windle, J. Popplewell and S.W. Charles, I.E.E. Transactions on Magnetics, Vol.11, 1367-1369, 1975.
2. 'The Magnetic Properties of Ferromagnetic Liquids Containing Iron Particles in Mercury', S.W. Charles and J. Popplewell. A paper presented at the Joint MMM-Intermag Conference, June 1976 and published I.E.E. Trans. on Magnetics, Vol. Mag-12, 795-797 (1976).
3. 'The Long Term Stability of Metallic Ferromagnetic Liquids', J. Popplewell, S.W. Charles and S.R. Hoon, A paper published September 1976 by the I.E.E. and delivered at the 2nd Conference on 'Advances In Magnetic Materials and their Applications'.
4. 'The Effect of a Particle Size Distribution on the Coercivity and Remanence of a Fine Particle System', R.W. Chantrell, J. Popplewell and S.W. Charles, a paper published in Physica 86-88B, p.1421, 1977 and delivered at the International Conference on Magnetism in Amsterdam; September 1976.
5. 'The Resistivity of Conducting Ferromagnetic Liquids Containing Iron Particles in Mercury', S.R. Hoon, J. Popplewell, S.W. Charles, a paper published in the I.E.E. Transactions on Magnetics vol Mag-14, No.5, p.981, (1978) and delivered at the Intermag Conference, Florence, May 1978.
6. 'The Preparation and Properties of a Stable Metallic Ferrofluid' S.W. Charles and J. Popplewell. Report on the Workshop on the Thermomechanics of Magnetic Fluids, Hemisphere Pub. Corp., Washington D.C.